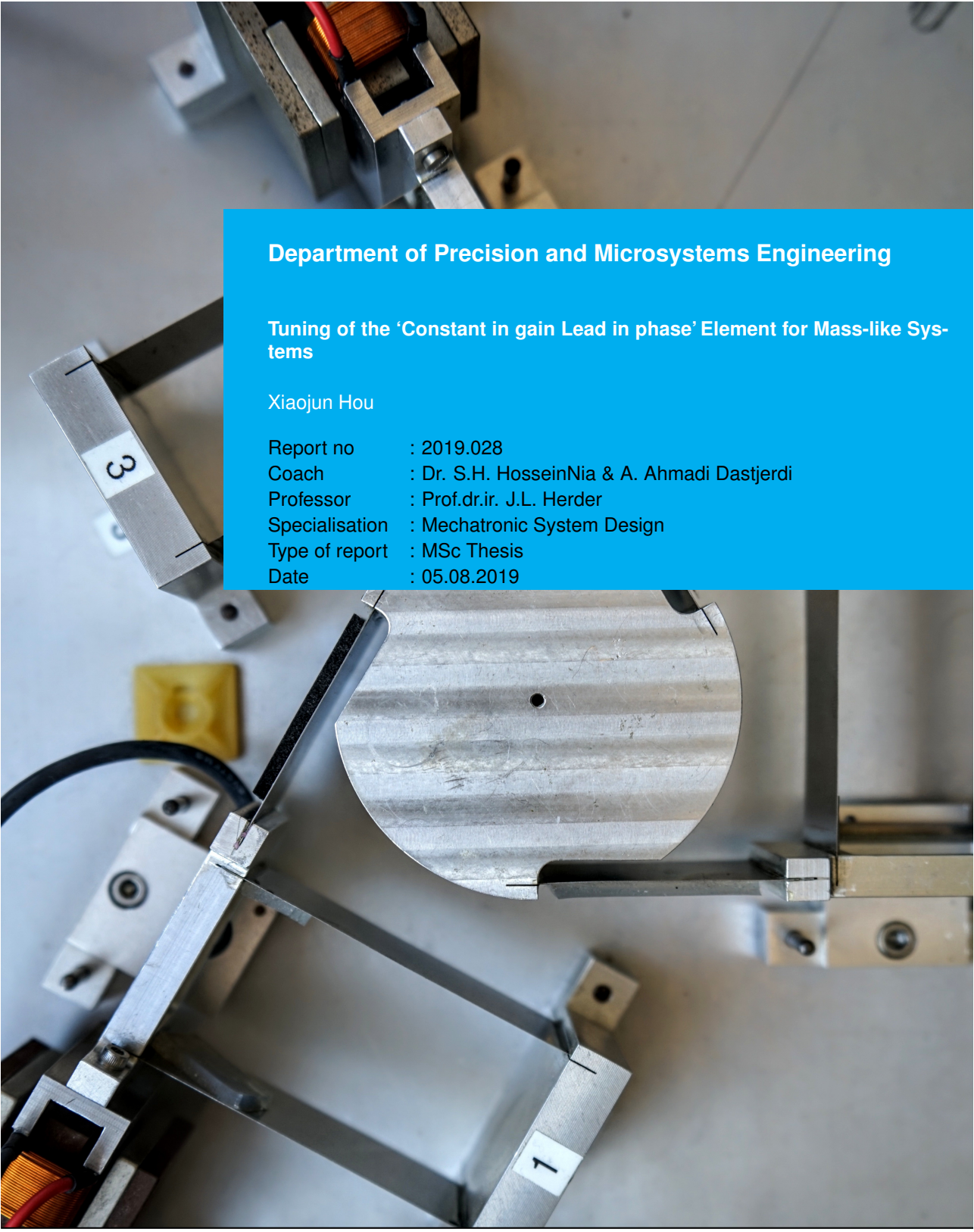

Department of Precision and Microsystems Engineering

Tuning of the 'Constant in gain Lead in phase' Element for Mass-like Systems

Xiaojun Hou

Report no	: 2019.028
Coach	: Dr. S.H. HosseinNia & A. Ahmadi Dastjerdi
Professor	: Prof.dr.ir. J.L. Herder
Specialisation	: Mechatronic System Design
Type of report	: MSc Thesis
Date	: 05.08.2019

TU Delft Delft University of Technology

Precision and Microsystems Engineering

Challenge the future

Tuning of the 'Constant in gain Lead in phase' Element for Mass-like Systems

by

Xiaojun Hou

For the degree of Master of Science in Mechanical Engineering
at Delft University of Technology,

to be defended publicly on Tuesday 27th August, 2019 at 2:00 pm

Student number:	4708326
Supervisor:	A. Ahmadi Dastjerdi
	Dr. S.H. HosseinNia
Thesis committee:	Prof.dr.ir. J.L. Herder (chairman)
	Dr. S.H. HosseinNia
	Dr. G.J. Verbiest
	Dr. N. Saikumar

An electronic version of this dissertation is available at
http://repository.tudelft.nl/.

TU Delft Delft University of Technology

Abstract

The development of the high-tech industry has pushed the requirements of motion applications to extremes regarding precision, speed and robustness. A clear example is given by the wafer and reticle stages that require rigorous demands like robust nanometer precision and high-speed motion profiles to ensure product quality and production efficiency. Industrial workhorse Proportional Integral Derivative (PID) has been widely used for its simple implementation and good performance. However, PID is insufficient to meet the ever-increasing demands in the high-tech industry due to its inherent constraints of linear controllers such as the waterbed effect. To overcome these fundamental limitations, researchers have turned to nonlinear controllers. Nevertheless, most of the nonlinear controllers are difficult to design and implement and thus are not widely accepted in the industry. Reset control is a nonlinear controller that is easy to implement and design since it maintains compatibility with the PID loop shaping technique using a pseudo-linear analysis tool named describing function method. However, the reset control as a nonlinear controller also introduces high order harmonics to the system that can negatively affect system performance by causing unwanted dynamics. Hence, describing function analysis as a linear approximation approach that only considers first harmonics is not accurate enough. Recently, a theory to analyze high order harmonics of nonlinear system in frequency domain termed higher order sinusoidal describing function has been developed, which enables the possibility to perform more precise analysis on reset systems.

The majority of research on reset control has focused on the phase lag reduction but a novel reset element proposed in literature termed ”Constant in gain, Lead in phase” (CgLp) is used to provide broadband phase compensation and has been shown to improve system performance. However, there is no systematic designing and tuning approach in literature such that the full advantage of CgLp elements is extracted. This work focuses on the tuning of the CgLp elements in order to obtain optimal performance. High order harmonics are also considered in the tuning analysis since they are critical to system performance due to the effect of unwanted dynamics.

When a group of CgLp elements are designed to provide pre-determined phase compensation at the crossover frequency, it is seen that the optimal tracking precision performance is always obtained with the case that has the highest frequency of third order harmonic peak and has almost the smallest magnitude of high order harmonics at low frequencies. Moreover, the second order CgLp controllers are observed to outperform the first order CgLp controller regarding tracking precision. On the other hand, configurations that have the lowest magnitude of third order harmonic at high frequency are found to have the best noise attenuation performance.

Contents

Preface

This thesis is made as a completion of the MSc Mechanical Engineering at the High-Tech Engineering (HTE) department of the TUDelft. Hereby, I would like to thank the following people who contribute directly or indirectly to this thesis. This accomplishment would not have been possible without them.

Ali Ahmadi Dastjerdi, thanks for being my daily supervisor during the project. You are always there whenever I ran into trouble or had a question about my research or writing.

Hassan HosseinNia, thanks for steering me in the right direction and guiding me to express my views more professionally. Your support and encouragement helped me a lot.

Niranjan Saikumar, thanks for helping me with Labview coding issues and comments on the thesis writing.

Jo Spronck, thanks for your valuable advice and advice on the Monday's meeting, which drove me to think about problems in pragmatic points of view.

Rob Luttjeboer and Bradley But, thanks for helping me with getting the "broken" encoder working again and other lab-related issues.

Friends at HTE department, the discussion on the regular meeting provided me with a source of inspiration and helped to improve my work.

My family, last but not the least I want to express my profound gratitude to my parents for providing me with unfailing support and continuous encouragement throughout my years of study.

Xiaojun Hou
Delft, July 2019

1

Introduction

The development of the high-tech industry has proposed ever-increasing requirements for the motion control. A typical representative is the lithography machine that is involved in the projection of the integrated circuit (IC) on wafers (Figure 1.1). As suggested by Moore's law, the size of transistors on ICs is getting smaller and so the industry has been challenged to make the die smaller (Figure 1.2). To maintain the quality of the die with ever-decreasing size, nanometer precision motion is a necessity. Meanwhile, the control strategy with high bandwidth enables faster motion and thus reduce production time.

Figure 1.1: Lithography machine. Image taken from ASML.

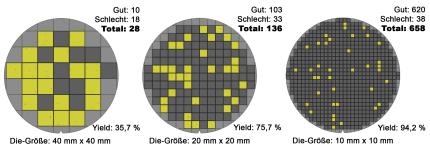

Figure 1.2: The change of die size on a wafer[1].

Proportional Integral Derivative (PID) control is the industrial standard for system control [2] and has been widely used in industry due to its simplicity and good performance regarding tracking, precision and robustness. During the designing of PID controllers, the loop shaping technique is used by engineers to tune the open loop frequency behavior. An open loop ideally has high gain at low frequencies to ensure good tracking performance and disturbance rejection and low gain at high frequencies to obtain better noise attenuation, while at the same time maintain sufficient phase at the bandwidth to ensure system robustness [3]. However, PID control is insufficient to meet the extreme requirements in the high-tech industry due to the fundamental limitations of linear controllers such as the waterbed effect and Bode's phase-gain relation [4]. The waterbed effect states that the decrease of sensitivity at one frequency range will inevitably lead to an increase at another.

1

Due to Bode's phase-gain relation, less phase lag over a larger range of frequencies around the bandwidth leads to a more robust system but also results in a worse magnitude shape, affecting the noise rejection at high frequencies and tracking performance at low frequencies. Therefore, there is trade-off between precision and robustness [5]. Nonlinear controllers have been used in literature to overcome these inherent constraints. Nevertheless, most of the nonlinear controllers are difficult to design and implement and thus are not widely accepted in the industry.

Reset control is a nonlinear controller that is easy to design and implement. A traditional reset controller resets the state to zero whenever its input crosses the zero point. In 1958, Clegg [6] proposed the first reset element which resets the state of an integrator to zero. If we use Describing Function (DF) tool, which considers only the first harmonic of the output of the controller of a sinusoidal wave input, the gain behavior of Clegg integrator (CI) is the same as the linear integrator while it produces 52° less phase lag than the simple integrator. Besides Clegg Integrator, other reset configurations have been developed to provide more design freedoms and applications: First Order Reset Element (FORE) [7] and Second Order Reset Element (SORE) [8]. Moreover, the advantages of reset control have been utilized to enhance the performance of several systems [9–14].

Although reset control has seen a lot of success over the years, it has mainly been used for its phase lag reduction advantage and has mainly been used as part of the integrator for this reason. However, N. Saikumar et. al. [15] proposed a novel reset element termed 'Constant-gain Lead-phase' (CgLp) which produces broadband phase lead while maintaining constant gain. This controller is made by combining the GFORE/GSORE with the first/second order linear lead filter. As a result of the design flexibility of reset elements, various combinations of tuning parameters could be used to provide the same open loop gain behaviour and equivalent phase compensation at the crossover frequency based on describing function analysis. However, it was seen that the improvement expected through describing function analyses was not achieved in some cases [16]. Hence, DF analysis is insufficient to perform frequency analyses for reset elements. Recently, Nuij [17] has extended describing function to higher order sinusoidal input describing functions (HOSIDF) for the analysis of these higher order harmonics of non-linear systems. With this tool, Heinen [18] developed HOSIDF for reset controllers and opened the possibility of more accurate analyses on reset controllers. Because of the design freedom even if the first harmonic matches in gain and phase compensation at the crossover frequency , the higher order harmonics are disparate. The motivation of this paper is to develop tuning guidelines of CgLp elements for so-called mass-like precision positioning systems using both describing functions and HOSIDF analyses.

2

Literature Review

This chapter presents the literature review in scientific paper format. Initially, the limitations of linear controllers are summarized. Then, the basis of reset control is introduced. Finally, the problem of unwanted dynamics in reset control along with the state of the art of reset strategies developed to handle this problem are represented and analysed.

A Review on the Application of Reset Control for Precision Mechatronics

Xiaojun Hou

***Abstract*— Proportional Integral Derivative (PID) controller is dominantly used for its ease of implementation and good performance regarding robustness and precision. However, it is bounded by its inherent limitation of the linear controller such as the waterbed effect. Reset controller as a type of nonlinear controller has shown the advantage of overcoming the fundamental limitation of linear controllers in literature. However, higher order harmonics are also introduced resulting in unwanted dynamics, affecting the overall performance of the system. This review paper discusses the issues in reset systems and the state of art of reset strategies to improve precision performance.**

***Index Terms*— Reset Control, Precision Positioning, Limit Cycles, Motion Control**

I. INTRODUCTION

Tracking, bandwidth and precision are three main motion control objectives for high-tech precision systems. A clear example is given by the wafer and reticle stages that require rigorous demands like robust nanometer precision and high-speed motion profiles to ensure product quality and production efficiency. PID controllers are widely used in the industry due to its simple implementation and good performance regarding robustness and precision [1]. However, due to the inherent limitations of the linear controller such as the waterbed effect and Bode's phase-gain relationship, linear PID is insufficient to meet the ever-increasing control requirements. With waterbed effect [2], improvement of disturbance rejection at one frequency inevitably leads to deterioration at another. With Bode's phase-gain relationship, additional phase margin around the bandwidth results in a more robust system but also leads to worse gain slope, affecting tracking and noise attenuation performance.

These fundamental limitations can be overcome by nonlinear controllers. Reset control is a simple nonlinear technique which resets the state when defined conditions are satisfied. Moreover, the frequency performance of the reset control can be analyzed using a linear approximation approach termed describing function (DF), which enables compatibility with linear PID controllers regarding loop shaping.

In 1958, Clegg [3] introduced the first reset controller, the Clegg Integrator(CI) which resets the state of the integrator to zero whenever the input crosses zero. Figure 1 shows the time response of reset integrator along with sinusoidal input. With describing function analysis, CI has 52° less phase lag compared with linear integrator while maintaining the same magnitude slope at all frequencies. Moreover, Horowitz et al. [4] introduced the First Order Reset Element (FORE) to achieve phase lag reduction at desired frequencies. More design freedoms are obtained in Second Order Reset Element(SORE) proposed by Hazelgar et al. [5]. On the other hand, the introduction of after reset variable leads to the development of Generalized First Order Reset Element GFORE [6] and Generalized Second Order Reset Element(GSORE) [7]. Recently, the introduction of fraction order dynamics [8], [9] to reset control further improved the design flexibility.

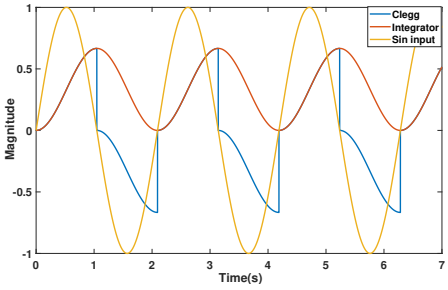

Fig. 1. Comparison of normal integrator and Clegg integrator with sinusoidal input

Reset control compensates the phase margin (PM) loss, or even increases the PM, reaches higher bandwidth, results in less overshoot or a faster settling time compared to linear controllers [10]. This advantage of reset controller has been used in many applications, from process control [11], [12], [13] to motion control [14], [16]. Despite the advantage, the resetting action also introduces higherorder harmonics that lead to unwanted dynamics such as limit cycles, which hinder the tracking and steady state performance of precision systems. In order to address this issue, various reset strategies have been developed [2], [18], [19]. This paper introduces the preliminaries of reset control and the problem of higher order harmonics along with the existent methods to deal with it.

The structure of the thesis is as follows, the fundamental limitations of the linear controller are summarized in section II. Section III gives the basis of a reset controller, describing functional analysis, stability and different types of reset elements. In section IV, an example is shown to discuss the problem of unwanted dynamics and the existing coping strategies are introduced. Finally, the conclusion is presented in the last section.

II. LIMITATION OF LINEAR CONTROLLERS

A. Phase-gain Relation

For a stable, minimum phase(no pole/zero in the in the right hand plane) system with open loop transfer function $G(s)$, a relation between phase$\angle G(j\omega)$ and magnitude$|G(j\omega)|$ exists:

$$\angle G(j\omega) \approx 90^{\circ} n(j\omega) \tag{1}$$

where n denotes the slope of magnitude:

$$n(j\omega) = \frac{d\log|G(j\omega)|}{d\log\omega} \tag{2}$$

Less phase lag over a larger range of frequencies around cross-over frequency leads to a more robust system, but also smaller slope of magnitude, affecting the noise rejection at high frequencies and tracking accuracy at low frequencies as shown in Figure 2. It is evident that a trade-off needs to be made between robustness and noise attenuation for the existence of phase-gain relation.

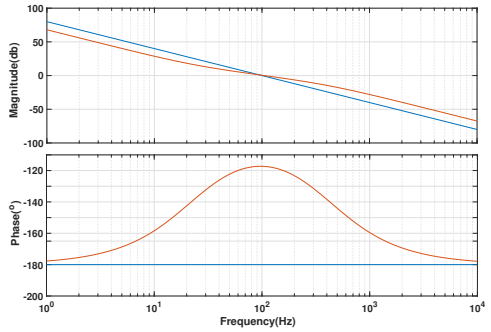

Fig. 2. Phase-gain relation diagram shows the trade-off between robustness and noise attenuation. Compared with the system represented by the blue line, the system represented by the red line has less phase lag at the crossover frequency, resulting in smaller slope of the magnitude. As a result, the magnitude at high frequency is magnified, deteriorating the noise attenuation performance.

B. Relation Between Sensitivity and Complementary Sensitivity Function

In a closed-loop system as shown in Figure 3, the sensitivity function, defined as the ratio of noise to output, implies the ability of the system to reject sensor and any additional noise. It could be described as:

$$S(s) = \frac{Y(s)}{N(s)} = \frac{1}{1 + P(s)C(s)} \tag{3}$$

The complementary sensitivity function, defined as the transfer from the reference to the output, describes the ability of the system to act as a servo system and is given by:

$$T(s) = \frac{Y(s)}{R(s)} = \frac{P(s)C(s)}{1 + P(s)C(s)} \tag{4}$$

Where $P(s)$ and $C(s)$ denote the transfer function of the plant and the controller. The constraint between sensitivity and complementary sensitivity function in a linear system can be described as:

$$S(j\omega) + T(j\omega) = 1, \forall\omega \tag{5}$$

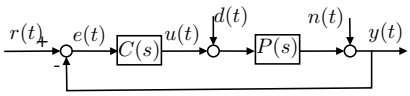

Fig. 3. Feedback loop with disturbance and noise

From (5) it is seen that both functions can not be close to one at the same frequency. There must be a trade-off between the properties of tracking performance and noise rejection at each frequency. If the peak of the complementary sensitivity function needs to be decreased, the sensitivity function will increase for that same peak frequency [23].

C. Waterbed Effect

For a linear system with no pole in the right half plane, the sensitivity function has the following property [2]:

$$\int_0^{\infty} \ln|S(j\omega)|d\omega = 0 \tag{6}$$

This equation states that the integral of the sensitivity function over the entire frequency range must equal zero. It implies that the decrease of sensitivity function at one frequency would inevitably lead to an increase at another, which is called the waterbed effect. Lower peak of sensitivity function $S(j\omega)$ leads to a more robust system, which is achieved by an increase at other frequencies. When the sensitivity increases at high frequencies, the noise attenuation is sacrificed. If the sensitivity is increased the low frequencies, the reference tracking performance will be affected for the existence of $S(j\omega)$ and $T(j\omega)$ relation as shown in (5).

III. RESET CONTROL

Reset control is a strategy that resets the controller states (or subset of states) to zero when some conditions hold [2]. It is the reset action that overcomes the limitation of linear controllers. In light of Figure 4, two more inputs are required than linear controllers which only need error $(e(t))$ input. Input $c(t)$ specifies the reset instants, which determine the condition to activate reset action. The after states‘ reset value, determining the degree of nonlinearity of the system, is set by $a(t)$.

Reset controllers (ΣR) as shown in Figure 5 have to parts: A basic linear part $C_b(s)$ and reset part $C_r(s)$. The integrated reset controller with zero crossing of $e(t) = 0$ as reset condition can be described as follows:

$$\begin{cases} \dot{x}(t) = A_r x(t) + B_r e(t) & \text{if } e(t) \neq 0 \\ x(t^+) = A_\gamma x(t) & \text{if } e(t) = 0 \\ u(t) = C_r x(t) + D_r e(t) \end{cases} \tag{7}$$

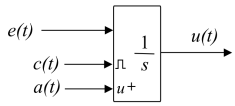

Fig. 4. Basic integrator with two additional inputs.Image courtesy [2]

where $x(t^+) \triangleq \lim_{s \to t+0} x(s)$. A, B, C and D represent the state matrix of the basic linear system. $e(t)$ is the error signal input to the system and $u(t)$ is the output. $x(t)$ is the state vector. First and the third equation denote the basic linear dynamics. When the reset condition is met, the reset action is triggered, represented by the second equation, and the reset matrix A_γ determines to which degree the state is reset.

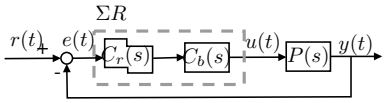

Fig. 5. Feedback loop with reset controller

A. Describing Function

Reset systems are nonlinear and transfer function no longer exists. A linear approximation method called describing function analysis is used to study the frequency behavior of reset control. The describing function method consists of replacing a nonlinear element within a system by an "equivalent" linear time-invariant system which is in some sense the best possible linear approximation of the nonlinear system [20]. The describing function is input dependent and sinusoidal excitation in usually chosen as input in the literature.

In [6], the sinusoidal describing function is given by Guo et. al. as:

$$G_{\mathrm{DF}}(j\omega) = C_r \left(j\omega I - A_r\right)^{-1} B_r \left(I + j\Theta_D(\omega)\right) + D_r \quad (8)$$

Where the notations are defined as follows:

$$\begin{aligned} \Theta_D(\omega) &= -\frac{2\omega^2}{\pi}\Delta(\omega)\left[\Gamma_r(\omega) - \Lambda^{-1}(\omega)\right] \\ \Lambda(\omega) &= \omega^2 I + A_r^2 \\ \Delta(\omega) &= I + e^{\frac{\pi}{\omega}A_r} \\ \Delta_r(\omega) &= I + A_\gamma e^{\frac{\pi}{\omega}A_r} \\ \Gamma_r(\omega) &= \Delta_r^{-1}(\omega) A_\gamma \Delta(\omega) \Lambda^{-1}(\omega) \end{aligned} \quad (9)$$

As mentioned previously, the describing function is a linear approximation of the nonlinear system, describing only the first harmonics of the output, and higher order harmonics are ignored. Since higher order harmonics are critical to precision positioning systems, it it necessary to take higher order harmonics into account as well.

An extension to higher order describing functions is realized by introducing the concept of the harmonics generator [22]. Recently, Heinen [21] derived the analytical expressions of higher order harmonics for reset controllers:

$$G(\omega, n) = \begin{cases} C_r(j\omega I - A_r)^{-1}\left(I + j\Theta_{D_r}(\omega)\right) B_r + D_r \\ \qquad\qquad \text{for } n = 1 \\ C_r(j\omega n I - A_r)^{-1} j\Theta_D(\omega) B_r \\ \qquad\qquad \text{for odd } n \geq 2 \\ 0 \qquad\qquad \text{for even } n \geq 2 \end{cases} \quad (10)$$

Where n denotes the order of harmonics.

B. Reset elements

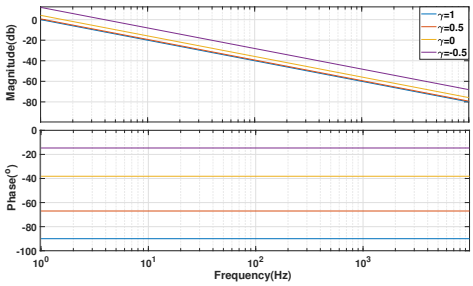

Fig. 6. Describing function of Clegg with various reset values

1) Clegg: An integrator is used as the basic linear system for Clegg Integrator. For Clegg the parameters of (7) become:

$$A_r = 0, B_r = 1, C_r = 1, D_r = 0, A_\gamma = \gamma$$

A reset value of $\gamma = 0$ leads to 52° less phase lag compared to a linear integrator. Figure 6 shows the describing function for changing reset values $\gamma \in [-1, 1]$, which is known as Generalized Clegg Integrator(GCI).

2) First Order Reset Element(FORE): Horowitz et al. [4] introduced the first order reset element(FORE) that resets the state based on first order low pass filter. The basic linear filter of FORE can be expressed as follows:

$$G(s) = \frac{1}{\frac{s}{\omega_r} + 1} \quad (11)$$

where ω_r denotes the crosover frequency of the low pass filter. The parameters of (7) are as follows:

$$A_r = -\omega_r, B_r = \omega_r, C_r = 1, D_r = 0, A_\gamma = \gamma$$

FORE provides the advantage of filter frequency placement that is not possible to achieve by Clegg and has been used for narrowband phase compensation in [24]. Figure 7 plots the describing function of Generalized First Order Reset Element(GFORE).

3) Second Order Reset Element(SORE): Considering the base linear system as (12), second order reset element, recently developed by Hazelgar et. al. [5], reset second order low pass filter or notch filter can be designed.

$$G(s) = \frac{\omega_r^2}{s^2 + 2\beta_r\omega_r s + \omega_r^2} \quad (12)$$

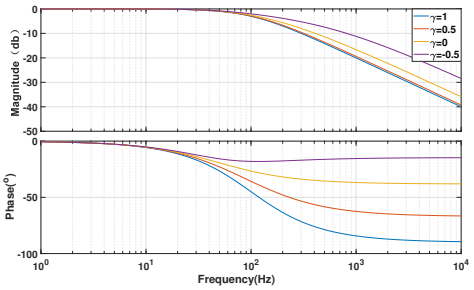

Fig. 7. Describing function of FORE with various reset values

And the parameters of (7) are given as:

$$A_r = \begin{bmatrix} 0 & 1 \\ -\omega_r^2 & -2\beta_r\omega_r \end{bmatrix}, B_r = \begin{bmatrix} 0 \\ \omega_r^2 \end{bmatrix}$$
$$C\_r = \begin{bmatrix} 1 & 0 \end{bmatrix}, D_r = [0]$$

Unlike Clegg and FORE, in which A_γ is a scalar, A_γ in SORE is a matrix given as:

$$A_\gamma = \begin{bmatrix} \gamma_1 & 0 \\ 0 & \gamma_2 \end{bmatrix}$$

Compared with FORE, SORE offers an extra degree of freedom to design reset element with the additional parameter damping ration β_r). Figure 8 shows the frequency response of SORE for various values of β_r. Change of β_r in SORE exerts little influence on the gain behavior while obtaining sharp phase change

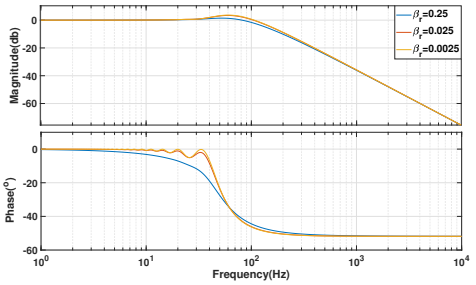

Fig. 8. Describing function of SORE with various damping cofficient,$A_\gamma = [0 \quad 0; 0 \quad 0]$, $\omega_r = 100Hz$

C. Stability Analysis

Consider a closed-loop system with reset controller as shown in Figure 9. The controller $\Sigma_(RC)$ is seperated into a part Σ_r whose states are reset and a part Σ_{nr} whose states are not reset. The following conditions must be satisfied for ensuring asymptotic stability [17].

Theorem1: *Let $V : \mathbb{R}^n \to \mathbb{R}$ be a continuously differentiable, positive-definite, radially unbounded function such*

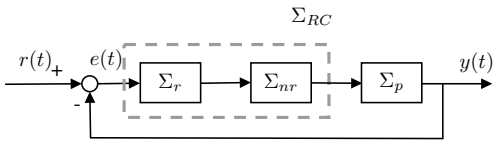

Fig. 9. Closed loop bock diagram of plant Σ_p controlled by Σ_{RC}

that

$$\dot{V}(\mathbf{x}) := \left(\frac{\partial V}{\partial \mathbf{x}}\right)^T A_{cl}\mathbf{x} < 0, \qquad if \quad \mathbf{e(t)} \neq 0 \tag{13}$$

$$\Delta V(\mathbf{x}) := V\left(A_R\mathbf{x}\right) - V(\mathbf{x}) \leq 0, \quad if \quad \mathbf{e(t)} = 0 \tag{14}$$

where

$$A_R = \text{diag}\left(A_\gamma, I_{nr}, I_{n_p}\right) \tag{15}$$

$$A_{cl} = \begin{bmatrix} A_r & B_r C_{nrp} \\ -B_{nrp}C_r & A_{nrp} \end{bmatrix} \tag{16}$$

Then the reset system is asymptotically stable.
where n_{nr} is the number of states of Σ_{nr} and n_p is the number of states in Σ_p A_{cl} is closed loop state matrix in which (A_r, B_r, C_r, D_r) are the state space matrices of Σ_r and $(A_{nrp}, B_{nrp}, C_{nrp}, D_{nrp})$ are the state space matrices of Σ_{nr} and Σ_p in series.

Furthermore, the reset system is said to be *quadratically stable* if it satisfies (15) and (16), for some $V(\mathbf{x}) = \mathbf{x}^\top P\mathbf{x}$ with $P > 0$. Following proposition will suffice for proving quadratic stability:

Theorem2: *There exist a constant $\beta \in \mathbb{R}^{n_r \times 1}$ and $P_\gamma \in \mathbb{R}^{n_r \times n_r}$,$P_\gamma > 0$ such that the restricted Lyapunov equation*

$$P > 0, A_{cl}^T P + P A_{cl} < 0 \tag{17}$$

$$B_0^T P = C_0 \tag{18}$$

has a solution for P, where C_o and B_o are defined by:

$$B_0 = \begin{bmatrix} 0_{n_{nrp} \times n_r} \\ 0_{n_r \times n_r} \\ I_{n_r} \end{bmatrix}, C_0 = [\beta C_{nrp} \quad 0_{n_r \times n_{nr}} \quad P_\gamma] \tag{19}$$

IV. Unwanted Dynamics and Existent Reset Strategies

A. Unwanted Dynamics in Reset Systems

Reset controllers can overcome the fundamental limitation of the linear controller but the resetting action introduces higher order harmonics which can negatively affect performance.. Moreover, since describing function is a linear approximation, unwanted dynamics cannot be indicated in the frequency domain. In the case of a reset integrator, for instance, the closed loop system does not have the same steady state properties as a linear integrator has [2]. The example below illustrates what is referred to aslimit cycles.

Considering a closed loop system shown in Figure 10, let $C(s)$ be a Proportional-Clegg integrator(PCI) controller, given by Equation 20 and the plant be $P(s) = \frac{1}{s+0.5}$.

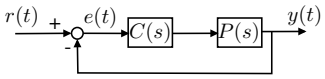

Fig. 10. Feedback closed loop

$$\mathrm{C}: = \begin{cases} \dot{x}(t) = e(t) & \text{if } e(t) \neq 0 \\ x\left(t^{+}\right) = 0 & \text{if } e(t) = 0 \\ u(t) = \frac{k_p}{\tau_i} x(t) + k_p e(t) & k_p = 2, \tau_i = 0.1 \end{cases} \quad (20)$$

The state of the controller is reset to zero whenever $e(t)$ crosses zero. The step response of the system is shown in Figure 11 compared with the response for the linear Proportional-Integrator(PI) controller without reset action. A system with PCI shows less overshoot due to the phase lag reduction provided by reset action. However, there is persisting oscillation at the set-point for the PCI system and thus steady state performance is deteriorated. The occurrence of this unwanted dynamics is caused by the mismatch of the after reset value $x_c\left(t^{+}\right) = 0$ and the steady state value of control signal of closed-loop linear system. The steady state control signal of a unit step reference equals to the inverse DC gain of the plant without the presence of disturbance. In this case steady state control $u_{ss} = 0.5$ and the corresponding after reset value of should be $x_c\left(t^{+}\right) = 0.5 \cdot \frac{\tau_i}{k_p} = 0.025$. Constantly resetting this to zero results in limit cycles .

B. Reset Strategies

Some reset control strategies in literature have bee developed to cope with this unwanted dynamics problem. These methods will be briefly discussed in this section.

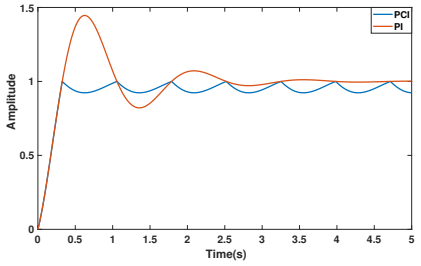

Fig. 11. Step response with limit cycles

1) PI+CI: PI+CI controllers [2] contains a parallel combination of linear integrator and Clegg integrator. The configuration is shown in Figure 12. An additional parameter $p_{reset} \in [0, 1]$ is introduced to make a trade-off between linear and Clegg integrator. By adjusting p_{reset}, the controller could either be dominated by PI or CI. Due to the reset action, PI+CI structure has a phase advantage compared with the linear PI controller. However, since this controller is a trade-off between linearity and nonlinearity, it does not use the full advantage of reset control and thus phase lag reduction is smaller compared with the CI controller.

To illustrate how PI+CI performs, consider a system in Figure 10 with the plant $P(s) = \frac{1}{s+0.5}$ controlled by PI+CI controller with $k_p = 2$ and $\tau_i = 0.1$.

Figure 13 gives the step response of system with different values of p_{reset}. It can be seen that the limit cycles are removed with $p_{reset} = 0.5$ and the settling time of PI+CI configuration is lesser than that of a normal PI configuration.

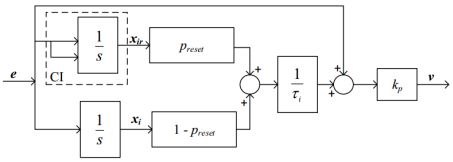

Fig. 12. PI+CI structure.Image courtesy [2]

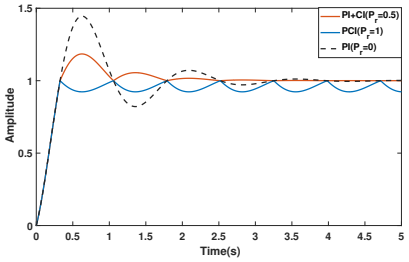

Fig. 13. step response of configurations with various p_{reset}

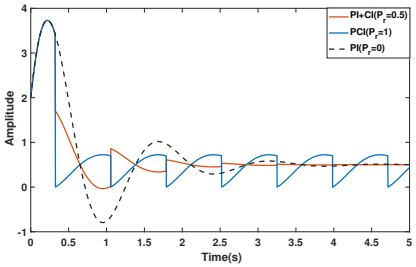

Fig. 14. Control signal of configurations with various p_{reset}

2) Reset with band: The reset with band strategy resets the state to zero once the error enters a defined band B_δ . B_δ is the tuning parameter to determine the width of the reset band [18]. This approach is expressed by:

$$\begin{cases} \dot{x}(t) = A_r x(t) + B_r e(t) & \text{if } (e(t), \dot{e}(t)) \notin B_\delta \\ x\left(t^{+}\right) = A_\rho x(t) & \text{if } (e(t), \dot{e}(t)) \in B_\delta \\ u(t) = \frac{k_p}{\tau_i} x(t) + k_p e(t) \end{cases} \quad (21)$$

where $B_\delta = (x, y) \in (R)^2 | (x = -\delta \wedge y > 0) \vee (x = \delta \wedge y < 0)$

This strategy is able to remove limit cycles in some cases but the system performance is dependent on the reset band, which makes the controller not robust for a practical system with model uncertainties and/or disturbance. To illustrate this, let the system shown in Figure 10 with the plant $P(s) = \frac{1}{s+0.5}$ and controller of (21) with $k_p = 2, \tau_i = 0.1$.

Figure 15 and Figure 16 show the step response and control signal of the system with reset band of $\delta = 0.1$ and $\delta = 0.2$. It can be seen that the limit cycles can be avoided only when the reset band is carefully selected. When a reset band of $\delta = 0.1$ is used, the limit cycles still exist together with steady state error. For the case $\delta = 0.2$, both limit cycles and steady state error are removed. But the system acts as a linear system inside the reset band, which makes the transient response slower than zero crossing reset strategy. Moreover, to the best of the author's knowledge there does not exist a systematic approach to determines the reset band in the literature.

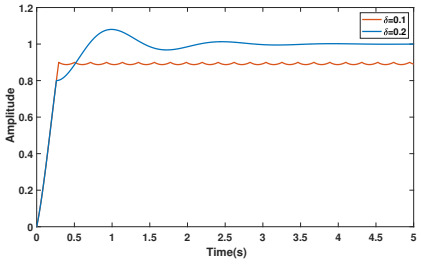

Fig. 15. Step response of reset band system with different reset band

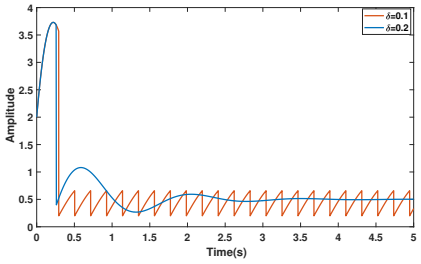

Fig. 16. Control signal of reset band system with different reset band

3) Fixed reset instants: Zheng et al. [15] extended the reset condition from zero crossing of error signal to fixed time instant and designed an improved PI reset controller for a positioning stage. Moreover, the after reset value $x_r\left(t_k^+\right)$ is determined at every reset instant by minimizing (22). The controller equations are given in (23).

$$J_k = e^T\left(t_{k+1}\right) P_0 e\left(t_{k+1}\right) + \dot{e}^T\left(t_{k+1}\right) Q_0 \dot{e}(tk+1) + \int_{t_k}^{t_{k+1}} e(s)^T P_1 e(s) ds \tag{22}$$

where P_0, P_1 and Q_0 are positive semidefinite tuning matrices and $e(t)$ is the error signal.

$$\begin{cases} \dot{x}_r = A_r x_r + B_r e, & t \neq t_k \\ x_r\left(t_k^+\right) = E_k x_p + F_k x_r + G_k r, & t = t_k \\ u = C_r x_r + D_r e \end{cases} \tag{23}$$

where A_r, B_r, E_k, F_k, G_k, C_r and D_r are appropriate dimensional constant matrices, x_r is the reset controller state vector, x_p are the plant states and r is the reference tracking signal.

This approach seems to be effective, but it can be restrictive in real applications, since the optimization depends on system matrices and tuning parameters and thus may be sensitive to model uncertainties. The thought of a constant reset instant is promising. A controller with a fixed reset instant might be more robust to noise since the reset action is not activated in zero crossing instants, which might be due to noise as well. However, there no procedure exists in the literature to determine reset instant interval Δt_k

4) Adaptive after reset variables: The idea of adapting the after reset value to steer it towards steady state value of the control signal has been used in [15] and [25]. Based on these works, Mark [19] proposed a robust adaptive reset controller which can reject limit cycles in case of model uncertainties and constant input disturbances. This strategy uses a similar configuration as the general PI reset controller with fixed reset instants (HosseinNia et al. [26], expressed by (24).

$$\begin{cases} \dot{x}_r(t) = e(t), & \text{if } t \neq t_k \\ x_r\left(t^+\right) = K\frac{\tau_i}{k_p} r(t) - \tau_i e(t), & \text{if } t = t_k \\ u_r(t) = \frac{k_p}{\tau_i} x_r(t) + k_p e(t) \end{cases} \tag{24}$$

In this algorithm, the limit cycles are detected by comparing the consecutive jump of the control signal. Once the limit cycle is present, K will be iteratively adapted to make the control signal converge to the steady state error until the limit cycle is removed.

V. Phase Compensation with Reset

The majority of the research in reset control was focused on the integrator and elimination of limit cycles. The main advantage obtained from reset was in phase lag reduction. On the other hand, works in [27] employ reset control on a different part of the PID framework. A PID controller is described as below:

$$G_{PID} = K_p \underbrace{\left(1 + \frac{\omega_i}{s}\right)}_{\text{Integrator}} \underbrace{\left(\frac{s}{\omega_d} + 1\right) / \left(\frac{s}{\omega_t} + 1\right)}_{\text{Tamed derivative}} \underbrace{\left(\frac{\omega_l}{s + \omega_l}\right)}_{\text{Low pass filter}} \tag{25}$$

where ω_i, ω_d, ω_t, ω_f are the corner frequency of integrator, lead, lag and low pass filter, respectively. K_p is chosen such that the open loop gain of describing function is unity at the bandwidth.

With the analysis of describing function, it is shown that the implementation of reset in tamed derivative and low pass filter outperform linear PID regarding bandwidth and precision. Based on work in [27], N. Saikumar et al. [7] proposed

a novel reset element termed "Constant-gain Lead-phase" (CgLp) which combines generalized reset elements (GFORE and GSORE) and the corresponding order of lead filter. This element was used to provide broadband phase compensation without affecting magnitude performance. Experimental results showed significant improvement in tracking and steady-state compared to Clegg Integrator based controllers and PID. However, it was shown that the improvement is dependent on the tuning of reset elements and that describing function of the CgLp-PID system cannot accurately represent closed-loop performance due to the effect of higher order harmonics [28]. While the effect of the higher order harmonics on performance is not as bad as seen in the previous cases with reset integrator, minor deviations are critical when dealing with precision positioning. Hence, tuning of CgLp considering higher order harmonics is necessary to make the best of reset elements.

VI. CONCLUSIONS

This review paper has presented an overview of reset control and proven the potential to overcome the fundamental limitations of linear controllers. Moreover, with the analysis of describing function, reset controllers can be designed using the industrial standard loop shaping techniques. However, higher order harmonics are also introduced due to resetting action and thus unwanted dynamics like limit cycles are present in system response. This downside of reset control hinders the performance of precision systems and strategies have been proposed to deal with the problem.

PI+CI, reset band, fixed reset instants and adaptive after reset variables are examples of methods studied in the literature to improve the performance of reset elements. Nevertheless, these strategies have some defects and are dependent on system characteristics. PI+CI provides a trade-off between linear and nonlinear control and thus the potential of reset controllers are not fully used. Although the reset band approach and fixed reset instants strategies have been shown to remove limit cycles, the performance depends on the reset band and reset instants. Unfortunately, there is no systematic approach in the literature to determine these parameters. Moreover, they are less robust against system uncertainties, which is also the problem for adaptive after reset variables strategy.

While most of the research has focused on the reset integrator, recent work on implementing reset within other parts of PID has been shown to provide higher precision and bandwidth. This strategy uses the nonlinear lead filter to provide phase compensation without damaging the magnitude performance.

The main issue regarding the study of reset control is that the describing function analysis cannot accurately represent system performance since it is a linear approximation and higher order harmonics are neglected. To obtain a more precise indication of a reset system performance, a comprehensive analysis needs to be developed.

REFERENCES

[1] K. J. Astrom and T. Hagglund, "The future of PID control,"*Control Engineering Practice* , vol. 9, no. 11, pp. 1163–1175, 2001.

[2] A. Baos and A. Barreiro,*Reset Control Systems* . Springer Publishing Company, Incorporated, 2013.

[3] Clegg J C. A nonlinear integrator for servomechanisms[J]. *Transactions of the American Institute of Electrical Engineers*, Part II: Applications and Industry, 1958, 77(1): 41-42.

[4] I. Horowitz and P. Rosenbaum, "Non-linear design for cost of feedback reduction in systems with large parameter uncertainty," *International Journal of Control*, vol. 21, no. 6, pp. 977–1001, 6 1975.

[5] Hazeleger, L., Heertjes, M., Nijmeijer, H. (2016, July). Second-order reset elements for stage control design. In 2016*American Control Conference (ACC)* (pp. 2643-2648). IEEE.

[6] Guo Y, Wang Y, Xie L. Frequency-domain properties of reset systems with application in hard-disk-drive systems[J]. *IEEE Transactions on Control Systems Technology*, 2009, 17(6): 1446-1453.

[7] Saikumar N, Sinha R K, HosseinNia S H. 'Constant in gain Lead in phase'element-Application in precision motion control[J]. arXiv preprint arXiv:1805.12406

[8] Saikumar, Niranjan, and S. H. HosseinNia. "Generalized fractional order reset element (GFrORE)." *9th European Nonlinear Dynamics Conference (ENOC)*. 2017.

[9] HosseinNia S H, Tejado I, Torres D, et al. A general form for reset control including fractional order dynamics[J]. *IFAC Proceedings Volumes*, 2014, 47(3): 2028-2033.

[10] O. Beker, C. V. Hollot, Y. Chait, and H. Han, "Fundamental properties of reset control systems," *IFAC Proceedings Volumes (IFAC-PapersOnline)*, vol. 15, no. 1, pp. 187–192, 2002

[11] Vidal A, Baños A. Reset compensation for temperature control: Experimental application on heat exchangers[J]. *Chemical Engineering Journal*, 2010, 159(1-3): 170-181.

[12] A. Davo and A. Banos, Reset control of a liquid level process, in 2013 IEEE 18th *Conference on Emerging Technologies Factory Automation (ETFA)* (IEEE, 2013) pp. 1–4

[13] F. Perez, A. Banos, and J. Cervera, "Periodic reset control of an in-line pH process," in *ETFA2011*. IEEE, 9 2011, pp. 1–4.

[14] Y. Guo, J. Zheng, M. Fu, Y. Wang, and L. Xie, "Development of an extended reset controller and its experimental demonstration," *IET Control Theory Applications*, vol. 2, no. 10, pp. 866–874, 2008.

[15] Zheng, J., Guo, Y., Fu, M., Wang, Y., Xie, L. (2007, October). Improved reset control design for a PZT positioning stage. In *2007 IEEE International Conference on Control Applications* (pp. 1272-1277). IEEE.

[16] Y. Li, X. Guo, and Y. Wang, "Phase lead reset control design with an application to HDD servo systems," in 9th *International Conference on Control, Automation, Robotics and Vision*, 2006, ICARCV '06, 2006

[17] Baños A, Carrasco J, Barreiro A. Reset times-dependent stability of reset control systems[J]. *IEEE Transactions on Automatic Control*, 2011, 56(1): 217-223

[18] A. Banos, S. Dormido, and A. Barreiro, "Limit cycles analysis of reset control systems with reset band," *IFAC Proceedings Volumes (IFAC-PapersOnline)*, vol. 3, no. PART 1, pp. 180–185, 2009.

[19] Ivens Mark,Robust Reset Control using Adaptive / Iterative Learning Control,2017,[Online]:http://resolver.tudelft.nl/uuid:736ac020-25f8-4e03-8a3e-46569e79974b

[20] Vidyasagar M. *Nonlinear systems analysis[M]*. Prentice Hall, 1978.

[21] K. Heinen, "Frequency analysis of reset systems containing a Clegg integrator: An introduction to higher order sinusoidal input describing functions",2018,[Online]:http://resolver.tudelft.nl/uuid:ccc37af2-fcbc-46ec-9297-afdc5c1ea4b5

[22] Nuij P, Bosgra O H, Steinbuch M. Higher-order sinusoidal input describing functions for the analysis of non-linear systems with harmonic responses[J]. *Mechanical Systems and Signal Processing*, 2006, 20(8): 1883-1904.

[23] MLA Freudenberg, Jim, Rick Middleton, and A. Stefanpoulou. "A survey of inherent design limitations." *Proceedings of the 2000 American Control Conference. ACC (IEEE Cat. No. 00CH36334)*. Vol. 5. IEEE, 2000.

[24] Li Y, Guo G, Wang Y. Nonlinear mid-frequency disturbance compensation in hard disk drives[C]//Proceedings of the 16th *International Federation Control Conference*. 2005: 3-8.

[25] Zheng J, Guo Y, Fu M, et al. Development of an extended reset controller and its experimental demonstration[J]. *IET Control Theory Applications*, 2008, 2(10): 866-874.

[26] HosseinNia S H, Tejado I, Torres D, et al. A general form for reset control including fractional order dynamics[J]. *IFAC Proceedings Volumes*, 2014, 47(3): 2028-2033.
[27] A. Palanikumar, N. Saikumar, and S. H. HosseinNia, “No More Differentiator in PID:Development of Nonlinear Lead for Precision Mechatronics,” 5 2018. [Online]. Available: http://arxiv.org/abs/1805.09703
[28] S.Yusuf."Tuning a Novel Reset Element through Describing Function and HOSIDF Analysis"2018 [Online] :http://resolver.tudelft.nl/uuid:2236e1f6-4dc5-4f7f-96da-fc83ead69445

3

Objective

3.1. Problem Definition

Reset control as a type of nonlinear controller has been shown the advantage of overcoming the fundamental limitation of linear controllers in literature. While most of the work on reset control has been focused on phase lag reduction, [15] proposed a novel reset 'Constant in gain Lead in phase' (CgLp) element that can provide broadband phase compensation and outperform linear PID controllers. However, it was shown that in some cases the improvement expected through describing function is not seen [16]. This is because reset control as a nonlinear element introduces higher order harmonics that cannot be indicated by describing function into the system which can negatively affect system performance. To take full advantage of the CgLp element and make it reliable for the high-tech industry, it is critical to include the higher order harmonics in design process. Based on this, the research goal of this thesis is:

To tune the 'Constant in gain Lead in phase' element such that the effect of high order harmonics is minimized and closed loop performance is optimized.

3.2. Research Approach

The research is conducted by the following approach:

- Use DF to design groups of CgLp elements that provide the specified amount of phase compensation at the crossover frequency.
- Use HOSIDF tool to analysis the open loop 3^{rd} harmonic frequency behavior for previously designed CgLp elements and identify features of these 3^{rd} harmonics.
- Study the closed loop performance of various configurations in Matlab simulation.
- Validate the applicability of the developed tuning guidelines on a precision positioning stage that can be identified as a mass spring damper system.

3.3. Thesis Outline

Chapter 1 discusses the challenge of motion control in the field of the high-tech industry and presents the motivation of this research. In Chapter 2, the states of art for reset control strategy are given. This chapter presents the formulation of the research objective and approach to reach the goal. The main work of this thesis, the study of developing tuning guidelines for CgLp elements is presented in Chapter 4 in scientific paper format. Finally, Chapter 5 gives the conclusion and recommendation for future research. More details on this research are given in the Appendices.

4

Tuning ‘Constant in gain Lead in phase ’ Elements for Mass-like Systems

This chapter is presented in the conference paper format. The performance of CgLp elements is investigated using DF and HOSIDF analysis. In this work, CgLp elements are designed to achieve the same first order harmonic behaviors and thus the performance deviation is dominantly affected by higher order harmonics. Through the analysis on third order harmonic behavior of various control configurations, tuning guidelines are developed and validated on a precision position stage.

Tuning of the 'Constant in gain Lead in phase' element for Mass-like Systems

Xiaojun Hou, Ali Ahmadi Dastjerdi, Niranjan Saikumar, S. Hassan HosseinNia

***Abstract*—Proportional Integral Derivative (PID) controllers are dominantly used in industry for their ease of implementation and simple structure. However, in the high-tech industry where utmost robustness and precision are required, PID controllers are bounded because of the fundamental limitations of linear controllers such as the waterbed effect. Thus, nonlinear controllers such as reset elements have been used to meet the new requirements of the high-tech industry. In literature, the Constant in gain Lead in phase (CgLp) element is a novel reset element developed to overcome the inherent limitations of linear PID controllers. However, a tuning guideline has not been proposed in the literature so far. In this paper, a recently developed method named higher-order sinusoidal input describing function (HOSIDF) is used to obtain greater insight into the frequency domain behaviour of this reset element and comparative analysis using tracking performance metrics is carried out for so-called mass-like systems controlled by CgLp. Based on these analyses, tuning guidelines for CgLp are developed and validated on a positioning stage. The results show the effectiveness of the developed simple tuning to be used by the high-tech industry.**

***Index Terms*—Reset Control, Motion Control, Describing Function, HOSIDF, CgLp**

I. Introduction

THE development of the high-tech industry has pushed the requirements of motion applications to extremes regarding precision, robustness and speed. Especially, for lithography machines, which are involved in manufacturing integrated circuits, the improvement in motion speed and precision has become more challenging nowadays. Proportional Integral Derivative (PID) has been widely used in industry for its ease of implementation and simple structure. However, the ever-increasing control requirements cannot be satisfied by these linear controllers due to fundamental limitations such as the waterbed effect [1]. To overcome the limitations of linear controllers, researchers have turned to nonlinear controllers such as reset control.

A traditional reset controller resets the state to zero whenever its input crosses the zero point. In 1958, Clegg [2] proposed the first reset element which resets the state of an integrator to zero. If we use Describing Function (DF) tool, which considers only the first harmonic of the output of the controller for a sinusoidal wave input, the gain slope of Clegg Integrator (CI) is the same as the linear integrator while it produces 52° less phase lag than the linear integrator. Besides CI, other reset configurations have been developed to provide more design freedom and applicability: Generalized First Order Reset Element (GFORE) [3] and Generalized Second Order Reset Element (GSORE) [4]. Apart from zero error crossing condition, other conditions like reset band [5] and fixed reset instants [6] have also been studied. Moreover, there are several techniques which are proposed to soften nonlinearities of reset controllers such as Partial Reset [5] and PI+CI [7] approaches. The advantages of reset control have been utilized to enhance the performance of heat exchangers [8], liquid level control systems [9] and precision positioning systems [10]–[14].

Although reset control has seen a lot of success over the years, it has mainly been used for its phase lag reduction advantage and has mainly been used as part of the integrator for this reason. However, N. Saikumar et. al. [15] proposed a novel reset element termed 'Constant-gain Lead-phase' (CgLp) which produces broadband phase lead while maintaining constant gain. This controller is made by combining the GFORE/GSORE with the first/second order linear lead filter. As a result of the design flexibility of reset elements, various combinations of tuning parameters could be used to provide the same open loop gain behaviour and equivalent phase compensation at the crossover frequency based on describing function analysis. However, it was seen that the improvement expected through describing function analyses was not achieved in some cases [16]. Hence, DF analysis is insufficient to perform frequency analyses for reset elements. Recently, Nuij [17] has extended describing function to higher order sinusoidal input describing functions (HOSIDF) for the analysis of these higher order harmonics of non-linear systems. With this tool, Heinen [18] developed HOSIDF for reset controllers and opened the possibility of more accurate analyses on reset controllers. Because of the design freedom even if the first harmonic matches in gain and phase compensation at the crossover frequency , the higher order harmonics are disparate. The motivation of this paper is to develop tuning guidelines of CgLp elements for so-called mass-like precision positioning systems using both describing functions and HOSIDF analyses.

The structure of the paper is as follows. Section II gives preliminaries on reset controllers. In section III, the tuning method is derived based on the analyses of DF and HOSIDF using the simulation results as basis for time domain performance. Then, section IV presents the experiment verification. Finally, conclusions and remarks for further study are provided in section V.

II. PRELIMINARIES

A. Definition of reset control

A reset controller can be generally defined by the differential inclusions as follows:

$$\Sigma_c := \begin{cases} \dot{x}(t) = A_r x(t) + B_r e(t) & \text{if } e(t) \neq 0 \\ x(t^+) = A_\gamma x(t) & \text{if } e(t) = 0 \\ u(t) = C_r x(t) + D_r e(t) \end{cases} \quad (1)$$

A_r, B_r, C_r and D_r are the state matrices of the base linear system. $e(t)$ and $u(t)$ are the error input and control output, respectively, and the reset action is triggered when the error crosses zero. Moreover, the resetting matrix A_γ determines states' value after reset action by which the nonlinearity of reset systems can be tuned by varying A_γ.

B. Describing function (DF) and higher order sinusoidal input describing function (HOSIDF)

Since reset systems are nonlinear, transfer functions no longer exist. A linear approximation method called describing function (DF) analysis is popularly used in literature to study the frequency behaviour of reset controllers. The sinusoidal input DF of reset systems defined by (1) is given as [5]:

$$G_{DF}(j\omega) = C_r(j\omega I - A_r)^{-1} B_r (I + j\Theta_D(\omega)) + D_r \quad (2)$$

where the notations are defined as follows:

$$\begin{aligned} \Theta_D(\omega) &= -\frac{2\omega^2}{\pi}\Delta(\omega)\left[\Gamma_r(\omega) - \Lambda^{-1}(\omega)\right] \\ \Lambda(\omega) &= \omega^2 I + A_r^2 \\ \Delta(\omega) &= I + e^{\frac{\pi}{\omega}A_r} \\ \Delta_r(\omega) &= I + A_\gamma e^{\frac{\pi}{\omega}A_r} \\ \Gamma_r(\omega) &= \Delta_r^{-1}(\omega) A_\gamma \Delta(\omega) \Lambda^{-1}(\omega) \end{aligned} \quad (3)$$

To include high order harmonics and obtain a more reliable frequency description of reset system, HOSIDF is obtained in [4], [18] as :

$$G(\omega, n) = \begin{cases} C_r^T(j\omega n I - A_r)^{-1} j\Theta_D(\omega) B_r & \text{for odd } n \geq 2 \\ 0 & \text{for even } n \geq 2 \end{cases} \quad (4)$$

where n is the order of harmonics.

Based on the above equations, harmonics of the FORE with a corner frequency of ω_n and its linear base are depicted as in Figure 1. Based on the first harmonics, it can be seen that the reduction of phase lag is obtained without significant change of magnitude but with a small shift of corner frequency. Moreover, it is worthy to note that the behaviour of 5^{th} and higher harmonics are similar to that of 3^{rd} harmonic and the only difference is that the magnitude decreases with increasing order. On this account, we use only the 3^{rd} harmonic to analyze the effect of the higher order harmonics on closed loop performance. Note, the magnitude of higher order harmonics reach the peaks at a frequency around ω_n which is denoted by ω_p

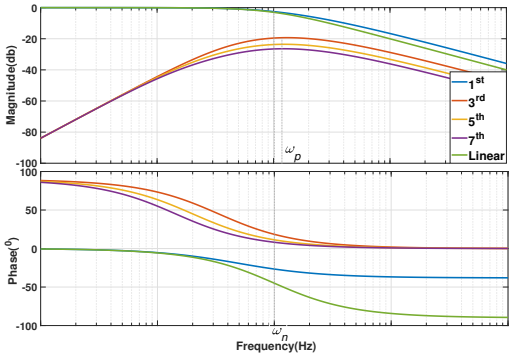

Fig. 1: Frequency behaviour of reset low pass filter, its linear base and high order harmonics.

C. New error sensitivity for reset systems

In linear systems, the sensitivity function from reference signal ($r(t)$) to error ($e(t)$) can be calculated by (5). This transfer function indicates the ability of the system to precisely follow the reference signal.

$$S(s) = \frac{e}{r} = \frac{1}{1 + G(s)C(s)} \quad (5)$$

$G(s)$ and $C(s)$ are the transfer function of the plant and controller, respectively.

For nonlinear controllers, $C(s)$ can be substituted with DF of the controller to analyze tracking performance. However, it is not accurate enough to predict the precision tracking performance of the controller since high order harmonics are neglected. To obtain a better indicator for reset systems, considering a sinusoidal reference $r = r_0 sin(\omega t)$, a new sensitivity function (S_σ) is defined as:

$$\forall \omega : S_\sigma(\omega) = \frac{\max_{t \geq t_{ss}}(|e(t)|)}{|r_0|} = \frac{\max_{t \geq t_{ss}}(|r(t) - y(t)|)}{|r_0|} \quad (6)$$

where $y(t)$ is the system output, t_{ss} indicates the settling.

D. CgLp

In [15], CgLp is introduced as a phase compensator by combining GFORE or GSORE with corresponding order of lead filters. The first order CgLp is defined as follows:

$$C_{CgLp1}(s) = \frac{1}{\frac{s}{\omega_{r\alpha}} + 1} \gamma \frac{\frac{s}{\omega_r} + 1}{\frac{s}{\omega_t} + 1} \quad (7)$$

where γ is a parameter that tunes after reset value and determines the matrix A_γ. ω_r and ω_t are the starting and taming frequencies of linear lead filter. $\omega_{r\alpha} = \omega_r/\alpha$ is the corner frequency of the reset element and α is the correction factor accounting for the shift of corner frequency to ensure constant gain of CgLp elements. The values of α determined by γ are summarized in Table I [15]:

TABLE I: Correction factor α of first order CgLp.

γ	αa	γ	α
0.9	1.0	-0.1	1.60
0.8	1.01	-0.2	1.81
0.7	1.02	-0.3	2.09
0.6	1.04	-0.4	2.47
0.5	1.07	-0.5	3.01
0.4	1.11	-0.6	3.85
0.3	1.16	-0.7	5.26
0.2	1.23	-0.8	8.19
0.1	1.32	-0.9	16.71
0	1.44		

Similarly, the second order CgLp can be defined as below:

$$C_{CgLp2}(s) = \frac{1}{\left(\frac{s}{\omega_{r\alpha}}\right)^2 + 2s\frac{\beta_{r\alpha}}{\omega_{r\alpha}} + 1} \frac{\left(\frac{s}{\omega_r}\right)^2 + 2s\frac{\beta_r}{\omega_r} + 1}{\left(\frac{s}{\omega_t} + 1\right)^2} \quad (8)$$

where $\omega_{r\alpha} = \omega_r/\alpha_1$ and $\beta_{r\alpha} = \beta_r/\alpha_2$ are the corner frequency and damping ratio of the reset element, respectively. α_1 and α_2 (Table II) are correction factors considering the shift of corner frequency and adjustment of damping ratio to guarantee constant gain of second order CgLp elements (Only $\beta_{r\alpha} = 1$ is investigated in this paper).

TABLE II: Correction factors α_1 and α_2 of second order CgLp.

γ	α_1, α_2	γ	α_1, α_2
0.9	0.99, 1.03	-0.1	1.52, 1.63
0.8	0.98, 1.05	-0.2	1.92, 1.91
0.7	0.96, 1.07	-0.3	2.43, 2.10
0.6	0.94, 1.07	-0.4	3.11, 2.21
0.5	0.92, 1.06	-0.5	4.23, 2.49
0.4	0.90, 1.03	-0.6	5.89, 2.76
0.3	0.89, 1.00	-0.7	8.66, 3.01
0.2	0.93, 1.02	-0.8	14.11, 3.2
0.1	1.03, 1.14	-0.9	30.09, 3.28
0	1.23, 1.36		

Figure 2 shows DF and HOSIDF behaviour of first order CgLp confgurations that are used to provide the same amount of phase compensation at pre-determined frequency ω_c. In this thesis, we will analyze the 3^{rd} harmonic of the reset part in the CgLp elemtent instead of the entire CgLp implementation since it is this reset part that introduces higher order harmonics and the 3^{rd} harmonics behaviour is more straightforward. From the perspective of the frequency behaviour, the phase compensation provided by the CgLp element starts from $\omega_{r\alpha}$ and reaches the maximum level which is determined by γ at higher frequencies. Hence, the phase compensation provided by CgLp elements at ω_c of a system can be defined as $\theta(\omega_r, \gamma)$, which is a function of ω_r and γ. By tuning ω_r and γ, equivalent phase compensation θ can be obtained and constant gain is maintained according to DF analysis. From the figure of HOSIDF behaviour, it is seen that the 3^{rd} harmonics are quite different even though first harmonic is very similar. It is observed that the peaks magnitude of 3^{rd} harmonic increase when lowering γ and the sequence of magnitude for various configurations is distinctive at low and high frequencies due to the tuning of ω_r. To summarize, CgLp elements can be flexibly tuned by varying γ and ω_r to achieve required amount of phase

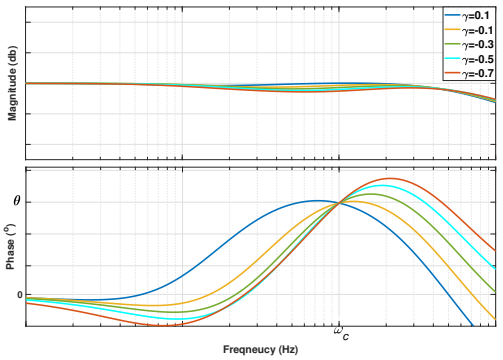

(a)

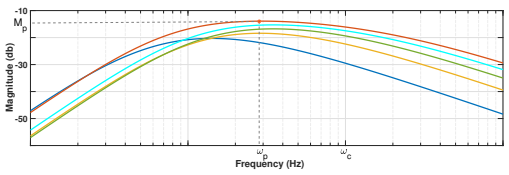

(b)

Fig. 2: (a): DF of first order CgLp configurations with various ω_r and γ that provode θ degrees phase compensation at ω_c ; (b): 3^{rd} order HOSIDF of the reset part in CgLp elements.

compensation. Moreover, the behaviour of 3^{rd} harmonic is also determined by tuning parameters.

E. Motivation of Cglp tuning

CgLp has proved the advantage of overcoming the fundamental constraints of linear controllers. However, it was seen that in some cases, the improvement expected through describing function analysis was not seen [16]. This is because performance prediction is based on DF analysis and does not take HOSIDF into account. Hence, it is of importance to understand how higher order harmonics affect the system performance. When CgLp elements are designed to provide the same amount of θ at the crossover frequency, we will assume that the discrepancy in system performance is caused by higher order harmonics since the first harmonic is equivalent based on the DF analysis. The motivation of this paper is to tune the CgLp element such that we minimize the effect of higher order harmonics and enhance the tracking performance of CgLp. The main parameters used in this paper are summarized in Table III.

III. TUNING GUIDELINES

This section presents the process of developing CgLp tuning guidelines in simulation. Once the CgLp elements are designed to provide the same amount of θ, it is assumed that the case with optimal tracking performance is affected the least by higher order harmonics. In this paper, the tracking is evaluated based on new error sensitivity (S_σ). Then, the

TABLE III: Some parameters used in this paper.

Parameters	Meaning	Units
γ	Variable to tune after reset value	\
$\alpha, \alpha_1, \alpha_2$	Coefficients to ensure constant gain in CgLp	\
b	Variable to tune ω_r of CgLp	\
ω_r	Corner frequency of lead filter in CgLp	Hz
$\omega_{r\alpha}$	Corner frequency of FORE / SORE in CgLp	Hz
ω_p	Frequency at which 3^rd harmonic reach peak	Hz
ω_c	Crossover frequency where θ phase is provided	Hz
θ	Phase compensation achieved at crossover frequency	$^\circ$
M_p	Peak Magnitude of 3^{rd} harmonic	db

relation between open loop 3^{rd} harmonic behaviour and closed loop tracking performance is established, which leads to the tuning guidelines.

A. Designing of controllers

Due to the design flexibility of CgLp configurations, several groups of first and second order CgLp elements can be designed to produce θ $(20^\circ, 30^\circ, 40^\circ, 50^\circ)$ phase compensation at ω_c by varying γ and ω_r. Crossover frequency of the system ω_c is set as $100Hz$. The value of γ is chosen from -0.9 to 0.9 with an increment of 0.1. And $\omega_r = \omega_c/b$ where b is used to obtain the corner frequency of CgLp elements and is determined by γ and θ. All in all, the parameters for all configurations can be summarized in Table IV and V. Since the required amount of phase compensation cannot be obtained for all values of γ, some cells are left blank.

B. Closed loop precision performance

This subsection presents the closed loop performance of a system controlled by CgLp configurations designed in previous subsection. Without loss of generality and for simplicity, a mass system $P(s) = \frac{1}{ms^2}$ is controlled by first and second order CgLp. The closed loop block diagram of first order CgLp is shown in Figure 3.

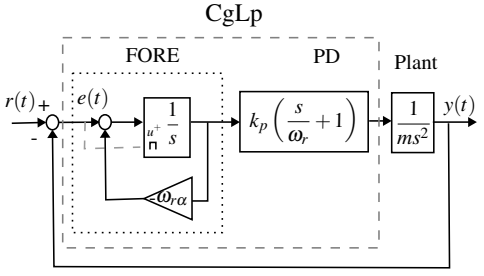

Fig. 3: Block diagram of the closed loop system with mass plant controlled by a first order CgLp compensator.

The performance of the system is evaluated based on tracking precision using the new error sensitivity S_σ mentioned in section II-C. We compare the S_σ behaviour of various configurations over frequencies smaller than $40Hz$ since tracking signals are generally composed of low frequency components in comparison to the crossover frequency. Then, the best configuration is selected upon S_σ. For instance, as shown in Figure 4, among configurations that provide 30° phase lead, CgLp1-8 and CgLp2-4 have optimal precision performance for first and second order CgLp, respectively. Similarly, the optimal configurations for 20°, 40° and 50° compensation can be obtained and all of the cases which provide optimal time domain performance within their group are highlighted in Table IV and V.

To understand how the open loop higher order harmonics affect the closed loop tracking performance, we characterize the 3^{rd} harmonic by the peak magnitude (M_p) that determines the level of nonlinearity and the frequency where the peak happens (ω_p) that affects the distribution of 3^{rd} harmonic over frequency domain (shown in Figure 2b). Values of M_p and ω_p are listed in Table IV and V. By comparison, it is found out that the scenarios that produce optimal tracking performance always have the largest value of ω_p within the group. Moreover, the optimal configurations from a tracking perspective, have almost the lowest magnitude of third harmonics at low frequency among the group. This relation between open loop 3^{rd} harmonic behaviour and closed loop performance provides a clue for the tuning of CgLp elements.

To investigate the noise attenuation performance of these CgLp elements. The reference signal is set as 0 and white noise with a maximum magnitude of $0.5\mu m$ is added to the feedback branch of the system shown in Figure 3. The configurations that have the best noise rejection are underlined in Table IV and V. It is found that these best cases correspond to configurations that have the lowest 3^{rd} harmonic at frequencies larger than ω_c.

Furthermore, although the aforementioned results are obtained based on investigation for a mass system, results of mass spring damper systems with a low resonance frequency and a high damping coefficient are expected to show the same conclusion. This is because CgLp controllers are usually used in combination of proportional integral (PI) controllers which shapes the open loop behaviour of a mass spring damper system that has a low resonance frequency into a mass-like system. And a high damping ratio ensures that the third harmonic is never higher than the first harmonic.

IV. VALIDATION

This section presents the experiments performed to investigate the performance of CgLp compensators on a precision positioning stage and to validate the previously obtained relation about open loop behaviour and closed loop performance on a mass spring damper system that has a small resonance frequency and a large damping ratio.

The precision positioning stage is shown in Figure 5. Three actuators are angularly spaced to actuate 3 masses (indicated by B1 B2 and B3) which are constrained by parallel flexures. These masses are connected to the central mass D through leaf flexures. Only actuator A1 is utilized to control the position of B1, so we have a SISO system. Mercury M2000 encoder is used the measure the position of mass B1 with a

TABLE IV: Parameters for first order CgLp configurations ($\omega_r = \omega_c/b, Hz$).

		20°			30°			40°			50°		
	γ	b	$\omega_p(Hz)$	$M_p(db)$	b	$\omega_p(Hz)$	$M_p(db)$	b	$\omega_p(Hz)$	$M_p(db)$	b	$\omega_p(Hz)$	$M_p(db)$
CgLp1-1	0.3	6.41	16.37	-22.63									
CgLp1-2	0.2	3.40	29.74	-21.40									
CgLp1-3	0.1	2.49	38.71	-20.31	6.80	14.18	-20.31						
CgLp1-4	0	2.02	44.78	-19.32	3.97	22.84	-19.32	25.82	3.51	-19.32			
CgLp1-5	-0.1	1.73	48.63	-18.41	2.92	28.72	-18.41	7.19	11.68	-18.41			
CgLp1-6	-0.2	1.51	50.79	-17.56	2.35	32.57	-17.56	4.45	17.20	-17.56	23.78	3.22	-17.56
CgLp1-7	-0.3	1.34	51.51	-16.77	1.98	34.78	-16.77	3.31	20.79	-16.77	8.21	8.38	-16.77
CgLp1-8	-0.4	1.19	51.00	-16.02	1.71	35.55	-16.02	2.66	22.85	-16.02	5.17	11.77	-16.02
CgLp1-9	-0.5	1.07	49.25	-15.30	1.50	34.96	-15.30	2.23	23.54	-15.30	3.84	13.69	-15.30
CgLp1-10	-0.6	0.95	45.90	-14.60	1.33	32.98	-14.60	1.92	22.81	-14.6	3.07	14.23	-14.62
CgLp1-11	-0.7	0.85	40.94	-13.91	1.18	29.49	-13.91	1.68	20.74	-13.91	2.57	13.53	-13.91
CgLp1-12	-0.8	0.75	33.72	-13.22	1.05	24.16	-13.22	1.48	17.12	-13.22	2.21	11.48	-13.22
CgLp1-13	-0.9	0.66	23.03	-12.47	0.94	16.26	-12.47	1.33	11.53	-12.47	1.94	8.59	-12.47

TABLE V: Parameters for second order CgLp configurations ($\omega_r = \omega_c/b$).

		20°			30°			40°			50°		
	γ	b	$\omega_p(Hz)$	$M_p(db)$	b	$\omega_p(Hz)$	$M_p(db)$	b	$\omega_p(Hz)$	$M_p(db)$	b	$\omega_p(Hz)$	$M_p(db)$
CgLp2-1	0.5	1.44	48.24	-22.74									
CgLp2-2	0.4	0.97	73.77	-21.14	1.61	44.48	-21.14						
CgLp2-3	0.3	0.83	87.98	-19.77	1.16	62.73	-19.77	1.39	42.65	-19.77	3.53	21.61	-19.77
CgLp2-4	0.2	0.75	94.17	-18.59	1.00	70.04	-18.59	1.35	52.26	-18.59	1.87	65.43	-18.58
CgLp2-5	0.1	0.68	94.18	-17.54	0.92	69.50	-17.54	1.23	52.31	-17.54	1.63	66.07	-17.53
CgLp2-6	0	0.59	92.14	-16.59	0.82	66.45	-16.59	1.36	49.25	-16.59	1.46	66.77	-16.60
CgLp2-7	-0.1	0.49	90.47	-15.73	0.69	64.75	-15.73	0.94	47.35	-15.73	1.26	67.54	-15.73
CgLp2-8	-0.2	0.40	89.06	-14.95	0.55	64.58	-14.95	0.75	47.18	-14.95	1.03	68.37	-15.00
CgLp2-9	-0.3	0.33	85.48	-14.22	0.45	63.67	-14.22	0.60	47.21	-14.22	0.83	34.65	-14.21
CgLp2-10	-0.4	0.28	79.93	-13.54	0.37	60.94	-13.54	0.49	45.92	-13.54	0.67	35.17	-13.54
CgLp2-11	-0.5	0.22	75.69	-12.90	0.29	58.15	-12.90	0.39	43.86	-12.90	0.53	35.77	-12.90
CgLp2-12	-0.6	0.18	69.84	-12.30	0.23	53.65	-12.30	0.31	40.32	-12.30	0.43	36.47	-12.30
CgLp2-13	-0.7	0.14	61.24	-11.73	0.19	46.44	-11.73	0.25	34.51	-11.73	0.35	24.84	-11.73
CgLp2-14	-0.8	0.11	48.04	-11.18	0.15	35.34	-11.18	0.21	25.79	-11.18	0.30	19.13	-11.18
CgLp2-15	-0.9	0.10	27.47	-10.66	0.14	19.42	-10.66	0.14	14.00	-10.66	0.27	10.00	-10.67

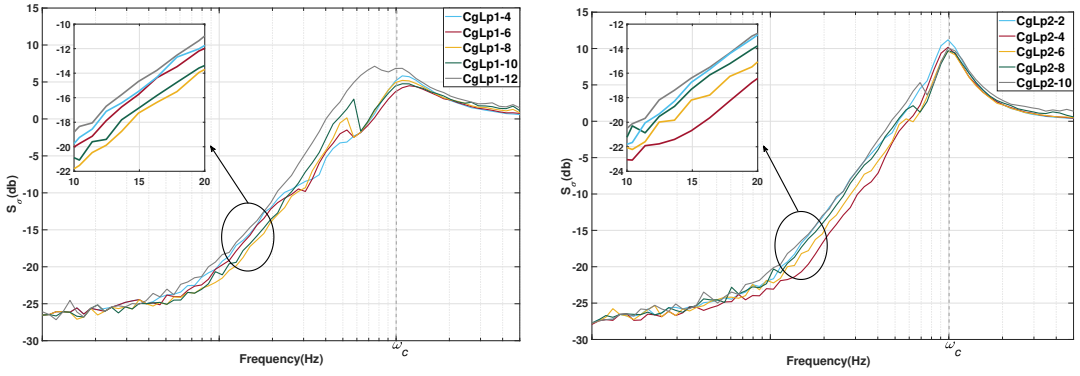

(a) First Order CgLp

(b) Second Order CgLp

Fig. 4: New error sensitivity S_σ of the mass system controlled by CgLp elements to achieve 30° phase compensation at crossover frequency.

resolution of 100nm. Controllers are implemented on FPGA NI CompactRIO.

Figure 6 shows the frequency response of the stage. The system can be approximated as a single mass spring damper system with estimated transfer function as follows.

$$P_{est}(S) = \frac{9602.5}{s^2 + 4.2676s + 7627.3} \tag{9}$$

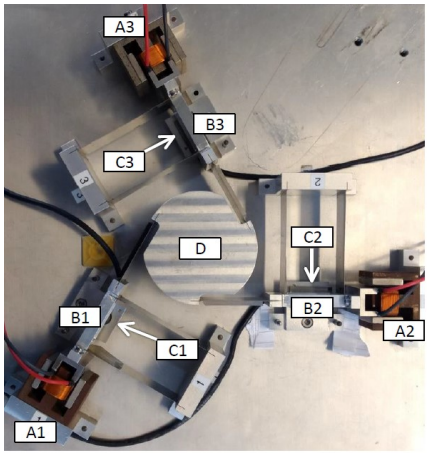

Fig. 5: Picture of precision positioning stage actuated voice coil actuators with encoder placed under mass of interest B1.

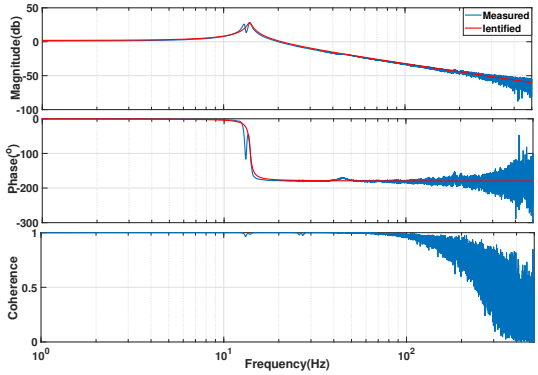

Fig. 6: Frequency response and estimated transfer function of the system

In order to validate the proposed relation, two control configurations (10) and (11) are implemented on the precision positioning stage.

$$G_1(s) = K_p \underbrace{\left(1 + \frac{\omega_i}{s}\right)}_{\text{Integrator}} \underbrace{\left(\frac{1}{\frac{s}{\omega_{r\alpha}} + 1}\gamma\right)\left(\frac{\frac{s}{\omega_r} + 1}{\frac{s}{\omega_f} + 1}\right)}_{CgLp_1} \tag{10}$$

TABLE VI: RMS and maximum steady state error for noise attenuation with system controlled by: a)First Order CgLp compensator, b)Second Order CgLp compensator

(a)

γ	20°		30°		40°	
	max(e(t))	RMS	max(e(t))	RMS	max(e(t))	RMS
0.3	10	3.35				
0.2	10	3.66				
0.1	23	7.67	8	2.40		
0	20	7.24	13	4.35	6	2.04
-0.1	45	19.98	26	10.60	8	2.64
-0.2	31	14.50	29	12.44	12	3.32
-0.3	55	29.34	35	17.00	29	13.38
-0.4	74	32.84	53	28.41	34	14.09
-0.5	150	43.93	63	29.12	58	30.15
-0.6	338	143.62	65	31.67	59	30.29

(b)

γ	20°		30°		40°	
	max(e(t))	RMS	max(e(t))	RMS	max(e(t))	RMS
0.5	11	3.31				
0.4	14	4.09	10	2.86		
0.3	15	4.41	11	3.87	7	2.48
0.2	19	5.44	16	3.78	14	5.21
0.1	19	7.55	16	3.84	13	4.41
0	26	10.03	14	4.35	15	4.84
-0.1	20	4.93	19	6.24	15	4.56
-0.2	19	5.39	19	6.19	14	5.40
-0.3	26	6.74	15	4.50	17	6.38
-0.4	29	9.77	20	7.74	24	7.45

and

$$G_2(s) = K_p \underbrace{1 + \frac{\omega_i}{s}}_{\text{Integrator}} \underbrace{\frac{1}{\left(\frac{s}{\omega_{r\alpha}}\right)^2 + 2s\frac{\beta_{r\alpha}}{\omega_{r\alpha}} + 1}\gamma \frac{\left(\frac{s}{\omega_r}\right)^2 + 2s\frac{\beta_r}{\omega_r} + 1}{\left(\frac{s}{\omega_f} + 1\right)^2}}_{CgLp_2} \tag{11}$$

The CgLp configurations of controllers (10) and (11) are tuned based on Table IV and V to produce 20°, 30°, and 40° degree phase at the crossover frequency. The crossover frequency of all designed controllers is set to 100Hz. Also, ω_i and $\omega_f$are tuned as $\omega_c/10$ and $5\omega_c$, respectively. All in all, we have six groups of control configurations and within each group the phase margin, the corner frequency and the type of CgLp element are the same. Moreover, the controllers are implemented with a sampling frequency of 20kHz.

The sinusoidal tracking experiments are carried out to validate proposed relation obtained by new error sensitivity S_σ analysis in the previous section. Since it is time-consuming to obtain the behaviour of S_σ over the entire frequency range, the maximum steady state errors of several sinusoidal input with frequencies of 5Hz, 10Hz, and 20Hz were used for performance analysis. Figure 7 and Figure 8 show the maximum steady state error of reference tracking and corresponding ω_p for each control configuration of first and second order CgLp. It is seen from the figures that the lowest value of maximum steady state error is obtained when the ω_p is the maximum. This is consistent with the analysis in the previous section.

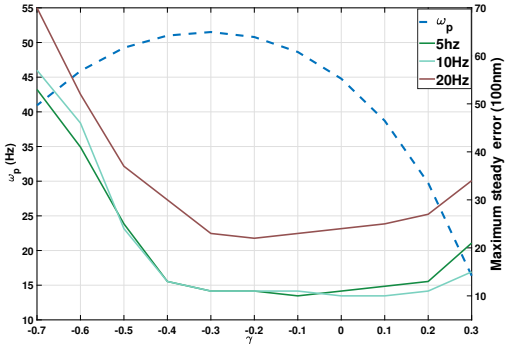

(a) 20° Phase Compensation

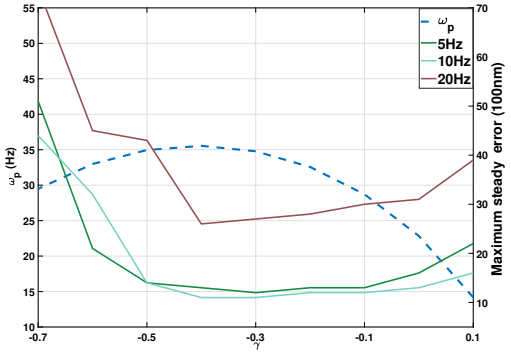

(b) 30° Phase Compensation

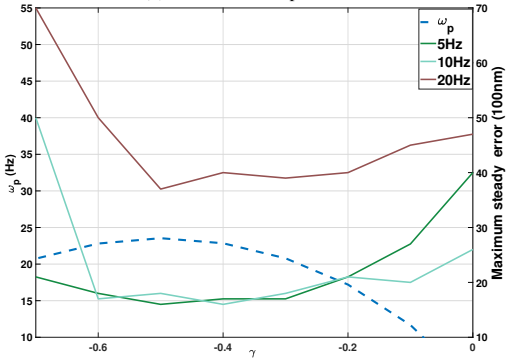

(c) 40° Phase Compensation

Fig. 7: Maximum steady state error of the system with various sinusoidal reference controlled by first order CgLp configurations.

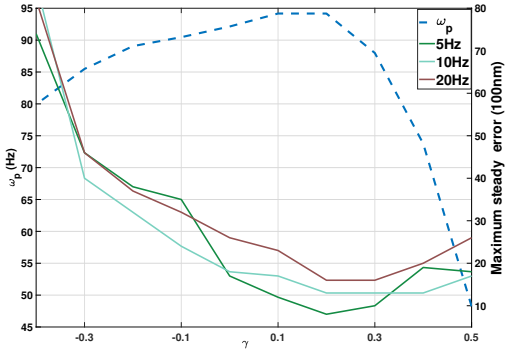

(a) 20° Phase Compensation

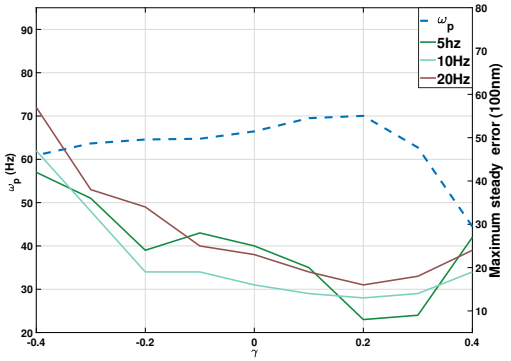

(b) 30° Phase Compensation

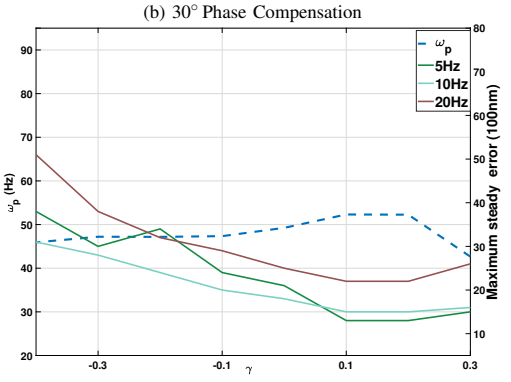

(c) 40° Phase Compensation

Fig. 8: Maximum steady state error of the system with various sinusoidal reference controlled by seoncd order CgLp configurations.

In the experiments of noise rejection, zero reference is used and additional white noise with a maximum magnitude of $0.5\mu m$ is applied to the feedback branch of the system as shown in Figure 3. Table VI shows the results for first and second order CgLp elements. It can be seen that the configurations with optimal noise attenuation performance within the group are consistent with cases indicated in Table I and V. Moreover, it is noteworthy that the optimal cases of first order CgLp outperform that of second order Cglp regarding noise attenuation.

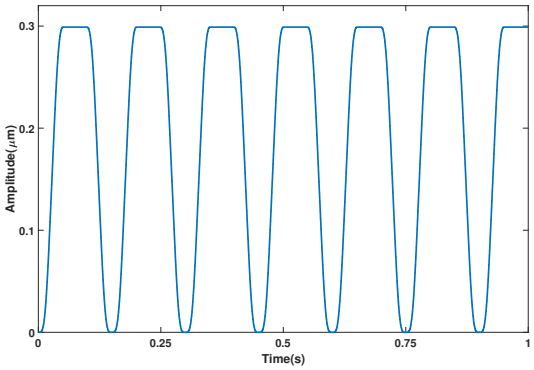

Fig. 9: Trajectory

Furthermore, the performance of a smooth trajectory (Figure 9) which is the combination of several sinusoidal waves with different frequencies is also investigated. TableVII shows the Root Mean Square (RMS) and maximum steady state error for each scenario. It is observed from the tables that the optimal performances regarding RMS and maximum steady state error are still obtained with reset values that produce a maximum ω_p. Moreover, it is interesting to notice that in most cases the optimal second order CgLp configuration outperforms that of first order CgLp. Based on the analyses in the previous section, this behaviour can also be explained by the fact that the ω_p of second order CgLp are larger than that of first order CgLp.

Based on these analyses, the tuning method can be summarized as:

(i) Use describing function to design a group of CgLp elements that provide the required phase lead as compensation at crossover frequency.

(ii) Check the frequency ω_p at which the 3^{rd} harmonic peak happens for each configuration using HOSIDF and choose the CgLp configuration that has the largest value of ω_p.

V. CONCLUSIONS

This paper has proposed a tuning guideline for Constant-gain Lead-Phase (CgLp) configurations for so-called mass-like systems. Several groups of CgLp controllers are designed to achieve the same amount of phase compensation and their open loop high order harmonics behaviour are investigated through high order sinusoidal describing function analysis (HOSIDF). Then, the closed loop precision performances for a mass system are evaluated by a new error sensitivity function which considers all orders of harmonics. It is found that the optimal tracking precision performances are obtained with cases that have the largest frequency of 3^{rd} harmonic peak (ω_p) and have almost the smallest magnitude of high order harmonics at low frequencies. On the other hand, configurations that result in the lowest magnitude of 3^{rd} harmonic at higher frequencies have the best noise attenuation performance. Although the guideline is developed through investigation on a mass system, it is also applicable for mass spring damper systems with low resonance frequency and high damping coefficient which behave like mass systems when applying proportional integral controller. Results are also validated by the experiment results of a mass spring damper precision position stage.

Overall, a straightforward tuning guideline of CgLp configurations considering both first and higher order harmonics is presented in this paper. This guideline improves the precision performance of CgLp controllers and can be widely applied in the high-tech industry. Although this thesis provides guidelines to minimize the effect of higher order harmonics, the exact relation between open loop higher order harmonics behaviour and closed loop performance is not known yet. Establishing a mathematical relation between open and closed loop frequency response could be part of future work.

TABLE VII: RMS and maximum steady state error for trajectory tracking with system controlled by: a)First Order CgLp compensator, b)Second Order CgLp compensator

(a)

γ	20°		30°		40°	
	max(e(t))	RMS	max(e(t))	RMS	max(e(t))	RMS
0.3	12	4.63				
0.2	9	2.85				
0.1	6	1.95	13	5.17		
0	7	2.14	8	2.92	31	12.51
-0.1	7	1.74	7	2.41	15	5.72
-0.2	7	2.11	7	2.54	12	4.29
-0.3	7	1.96	7	2.55	9	3.01
-0.4	22	9.95	7	2.23	10	3.26
-0.5	30	13.07	10	3.24	9	2.79
-0.6	39	15.50	27	8.14	12	4.19

(b)

γ	20°		30°		40°	
	max(e(t))	RMS	max(e(t))	RMS	max(e(t))	RMS
0.5	8	2.89				
0.4	4	1.32	5	1.72		
0.3	3	1.19	4	1.36	6	2.14
0.2	3	1.18	4	1.25	6	2.12
0.1	4	1.21	5	1.63	5	1.98
0	5	1.44	5	1.48	10	3.70
-0.1	7	1.92	6	1.70	11	3.67
-0.2	27	13.45	8	2.08	7	2.20
-0.3	40	18.03	17	5.77	8	2.30
-0.4	119	69.22	38	13.13	15	4.80

REFERENCES

[1] A. A. Dastjerdi, B. M. Vinagre, Y. Chen, and S. H. HosseinNia, "Linear fractional order controllers; a survey in the frequency domain," *Annual Reviews in Control*, 2019.

[2] J. Clegg, "A nonlinear integrator for servomechanisms," *Transactions of the American Institute of Electrical Engineers, Part II: Applications and Industry*, vol. 77, no. 1, pp. 41–42, 1958.

[3] I. Horowitz and P. Rosenbaum, "Non-linear design for cost of feedback reduction in systems with large parameter uncertainty," *International Journal of Control*, vol. 21, no. 6, pp. 977–1001, 1975.

[4] L. Hazeleger, M. Heertjes, and H. Nijmeijer, "Second-order reset elements for stage control design," in *2016 American Control Conference (ACC)*, pp. 2643–2648, IEEE, 2016.

[5] Y. Guo, Y. Wang, and L. Xie, "Frequency-domain properties of reset systems with application in hard-disk-drive systems," *IEEE Transactions on Control Systems Technology*, vol. 17, no. 6, pp. 1446–1453, 2009.

[6] J. Zheng, Y. Guo, M. Fu, Y. Wang, and L. Xie, "Improved reset control design for a pzt positioning stage," in *2007 IEEE International Conference on Control Applications*, pp. 1272–1277, IEEE, 2007.

[7] A. Baños and A. Barreiro, *Reset control systems*. Springer Science & Business Media, 2011.

[8] A. Vidal and A. Baños, "Reset compensation for temperature control: Experimental application on heat exchangers," *Chemical Engineering Journal*, vol. 159, no. 1-3, pp. 170–181, 2010.

[9] M. A. Davó and A. Baños, "Reset control of a liquid level process," in *2013 IEEE 18th Conference on Emerging Technologies & Factory Automation (ETFA)*, pp. 1–4, IEEE, 2013.

[10] L. Chen, N. Saikumar, and S. H. HosseinNia, "Development of robust fractional-order reset control," *IEEE Transactions on Control Systems Technology*, 2019.

[11] S. H. HosseinNia, I. Tejado, and B. M. Vinagre, "Fractional-order reset control: Application to a servomotor," *Mechatronics*, vol. 23, no. 7, pp. 781–788, 2013.

[12] N. Saikumar, R. K. Sinha, and S. H. HosseinNia, "Resetting disturbance observers with application in compensation of bounded nonlinearities like hysteresis in piezo-actuators," *Control Engineering Practice*, vol. 82, pp. 36–49, 2019.

[13] L. Chen, N. Saikumar, S. Baldi, and S. H. HosseinNia, "Beyond the waterbed effect: Development of fractional order crone control with non-linear reset," in *2018 Annual American Control Conference (ACC)*, pp. 545–552, IEEE, 2018.

[14] A. Palanikumar, N. Saikumar, and S. H. HosseinNia, "No more differentiator in pid: Development of nonlinear lead for precision mechatronics," in *2018 European Control Conference (ECC)*, pp. 991–996, IEEE, 2018.

[15] N. Saikumar, R. Sinha, and S. H. Hoseinnia, "constant in gain lead in phaseelement-application in precision motion control," *IEEE/ASME Transactions on Mechatronics*, 2019.

[16] Y.Salman, "Tuning a Novel Reset Element through Describing Function and HOSIDF Analysis." http://resolver.tudelft.nl/uuid:2236e1f6-4dc5-4f7f-96da-fc83ead69445, 2018.

[17] P. Nuij, O. Bosgra, and M. Steinbuch, "Higher-order sinusoidal input describing functions for the analysis of non-linear systems with harmonic responses," *Mechanical Systems and Signal Processing*, vol. 20, no. 8, pp. 1883–1904, 2006.

[18] K. Heinen, "Frequency analysis of reset systems containing a Clegg integrator: An introduction to higher order sinusoidal input describing functions." https://repository.tudelft.nl/islandora/object/uuid:ccc37af2-fcbc-46ec-9297-afdc5c1ea4b5?collection=education, 2018.

5

Conclusion

The objective of this thesis is:

To tune the 'Constant in gain Lead in phase' element such that the effect of high order harmonics is minimized and closed loop performance is optimized.

Based on this goal, the effect of control parameters on the phase compensation and higher order harmonics behaviors are investigated. By designing several groups of CgLp elements for a mass system that achieve equivalent amount of phase compensation at the crossover frequency and comparing their tracking performance, a relation between open loop 3^{rd} harmonic behavior and closed response is established. And the relation is extended to mass-behaving systems that have large damping ratio and small resonance frequency. Then, a precision positioning stage implemented with CgLp+PI controllers is used to validate the relation. And the results show that:

- From the perspective of sinusoidal and trajectory tracking, the configuration that has the largest value of 3^{rd} harmonic peak frequency and almost the smallest magnitude of 3^{rd} harmonic at low frequencies has the optimal performance, which is the case for both first and second order CgLp elements.
- From the perspective of noise attenuation, the configuration with the smallest magnitude of 3^{rd} harmonic at frequencies larger than the crossover frequency has the optimal performance.

Based on these, a tuning guideline using describing function and HOSIDF is given.

Following are the recommendations for further studies:

- This thesis mainly studies mass-behaving systems with low resonance frequency and large damping ratio. An investigation on mass spring damper system with a high resonance frequency and/or small damping ratio is also necessary.
- Although this thesis provides guidelines to minimize the effect of higher order harmonics, the exact relation between open loop higher order harmonics behaviors and

closed loop performance is not known yet. Establishing a mathematical relation between open and closed loop frequency response could be part of future work.

- While this work looks at which CgLp element is best for a given amount of phase compensation, it is still unknown what is optimal amount of phase compensation to be provided with CgLp and what amount should be provided by linear lead.

A

Coefficients

This appendix gives the processs to obtain coefficient b in Chapter 4 such that the required phase compensation (θ) is achieved at crossover frequency (ω_c). Consider a CgLp compensator that consists of reset part $C_r(s)$ and linear part $C_l(s)$, as shown by Figure A.1.

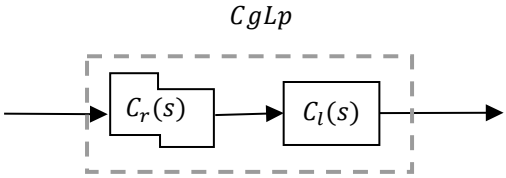

Figure A.1: CgLp compensator

To achieve θ degrees phase compensation at $\omega_c(Hz)$, the crossover frequency of the reset element ($\omega_r(Hz)$) can be obtained by the optimization equation as follows:

$$\min_{\omega_r} \quad |\theta - \angle(C_r(\gamma,\omega_r)C_l(\gamma,\omega_r))| \tag{A.1}$$

Subject to:

$$|\theta - \angle(C_r(\gamma,\omega_r)C_l(\gamma,\omega_r))| < 1$$
$$-1<\gamma<1$$

where:
for first order CgLp:

$$C_r(\gamma,\omega_r) = \frac{1}{\frac{\omega_c j}{\omega_{r\alpha}}+1}, \quad C_l(\gamma,\omega_r) = \frac{\omega_c j}{\omega_r} + 1 \text{ , } \omega_{r\alpha} = \omega_r/\alpha$$

or for second order CgLp:

$$C_r(\gamma,\omega_r) = \frac{1}{(\frac{\omega_c j}{\omega_{r\alpha}})^2 + 2\frac{\beta_{r\alpha}}{\omega_{r\alpha}}\omega_c j + 1}$$

A

$C_l(\gamma, \omega_r) = \left(\frac{\omega_c j}{\omega_r}\right)^2 + 2\omega_c j \frac{\beta_r}{\omega_r} +$, $\omega_{r\alpha} = \omega_r/\alpha_1$ and $\beta_{r\alpha} = \beta_r/\alpha_2$

Then,$b = \omega_c/\omega_r$

B

Simulation Results

This chapter presents the 3^{rd} harmonic behaviours of various CgLp configurations which is discussed in Section III of the paper in Chapter 4.

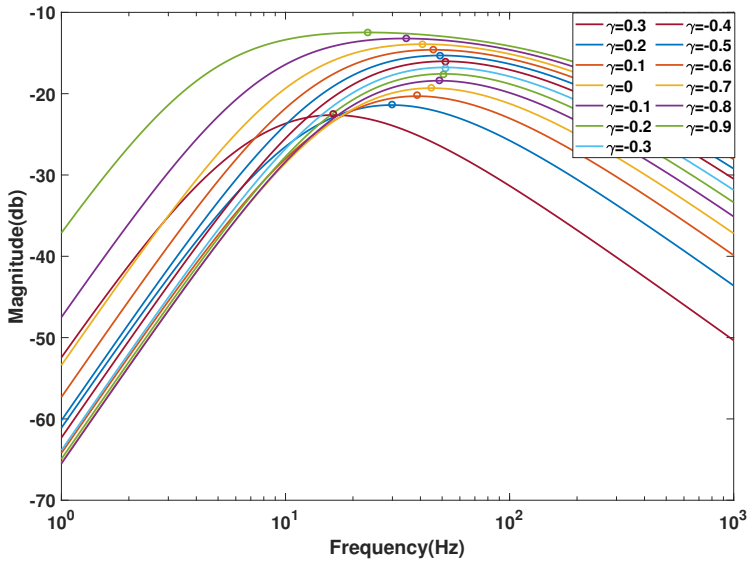

Figure B.1: Firsrt Order CgLp: 20°compensation

B

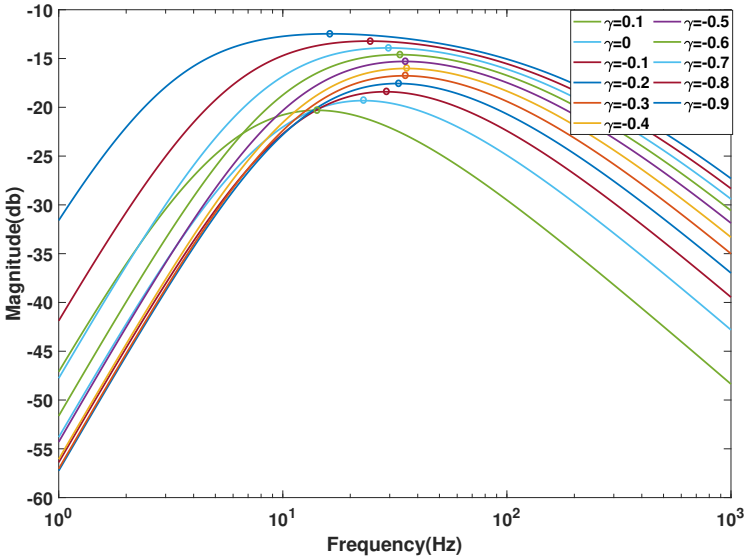

Figure B.2: Firsrt Order CgLp: 30°compensation

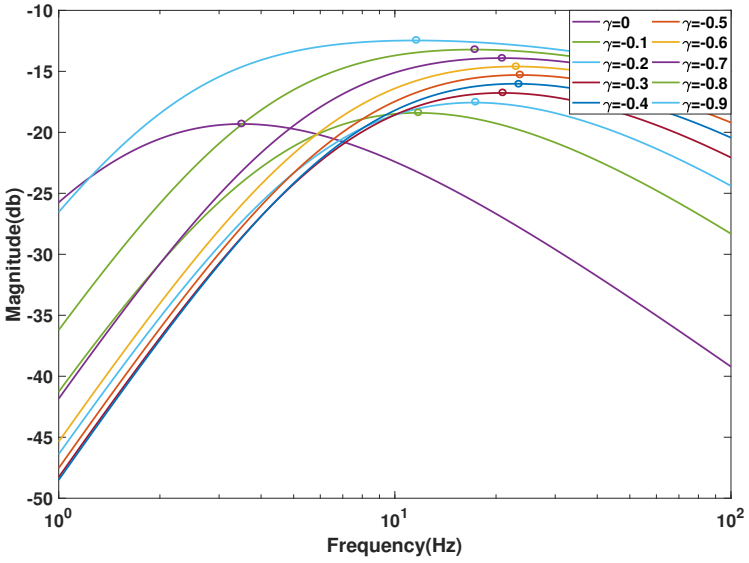

Figure B.3: Firsrt Order CgLp: 40°compensation

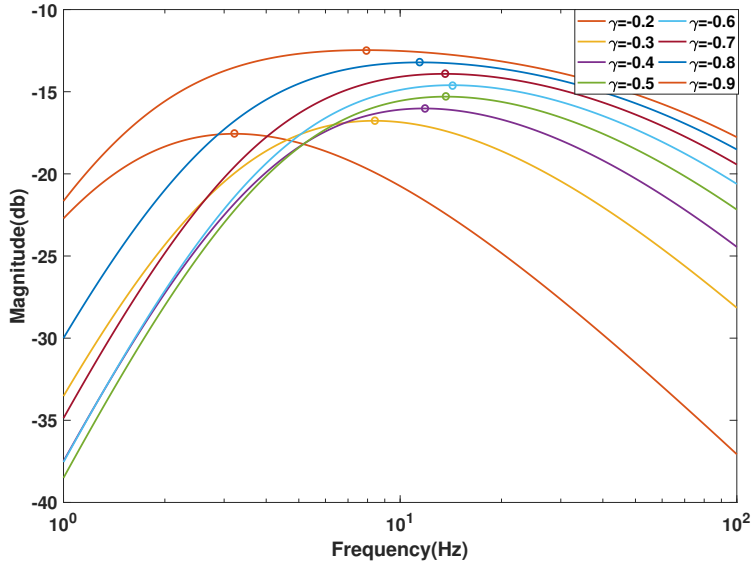

Figure B.4: Firsrt Order CgLp: 50°compensation

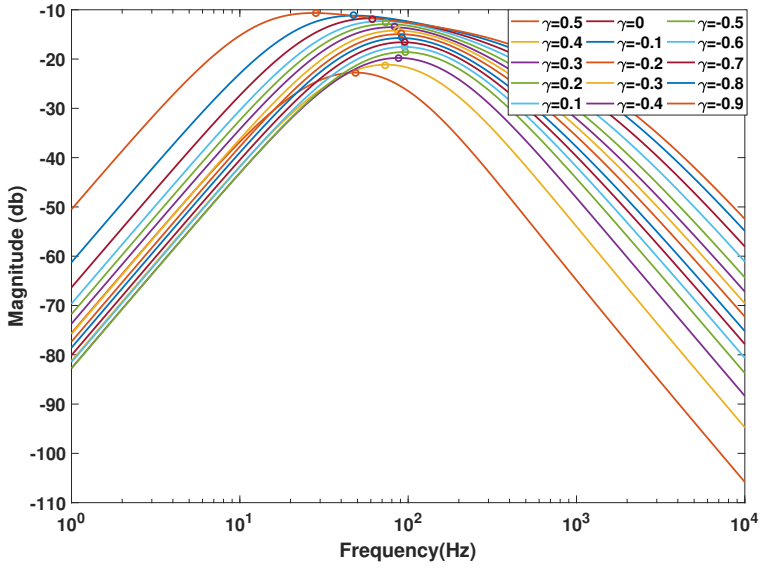

Figure B.5: Second Order CgLp: 20°compensation

B

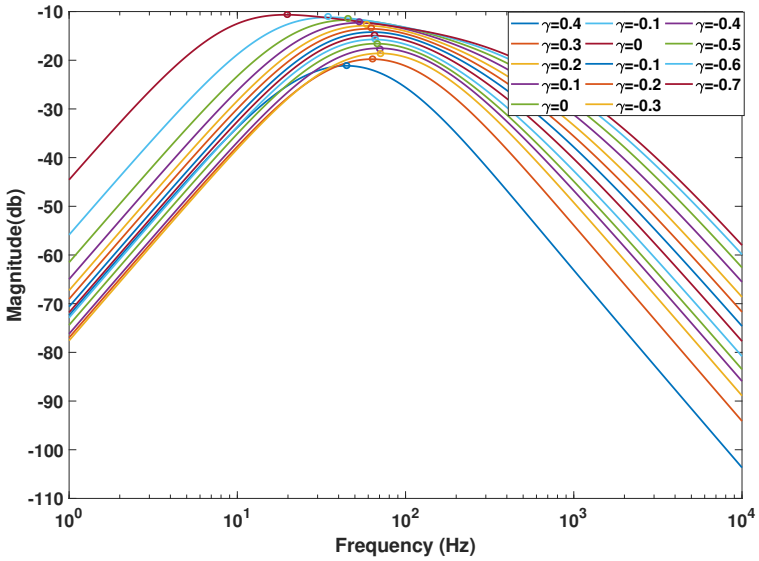

Figure B.6: Second Order CgLp: 30°compensation

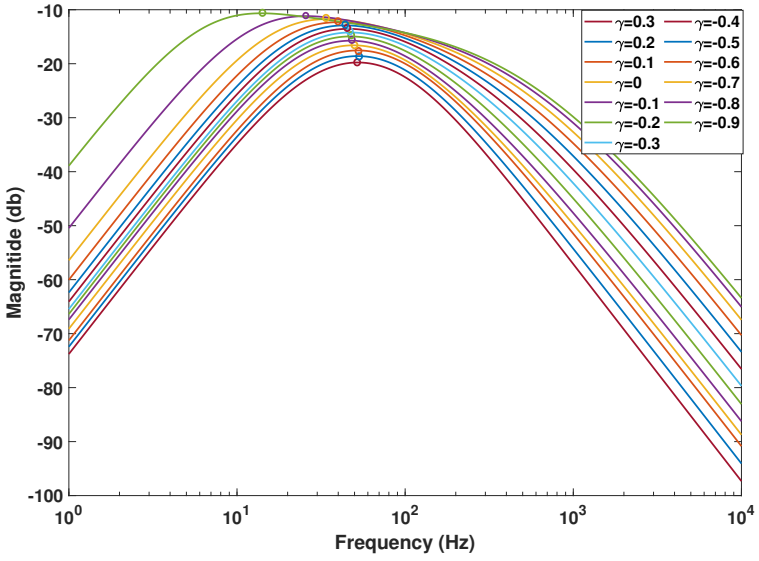

Figure B.7: Second Order CgLp: 40°compensation

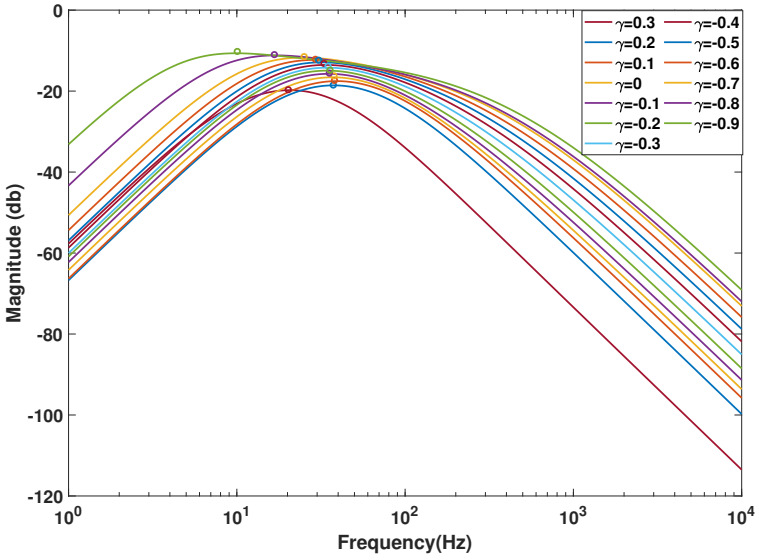

Figure B.8: Second Order CgLp: 50°compensation

C

System Overview

This chapter discusses the experimental setup that is used in this thesis. At first, the experimental setup is described. Then, the identification results for the whole system are presented.

C.1. Experiment Setup

The plant is a 3 degree of freedoms precision stage that consists of 3 angularly placed Lorentz actuator (A_1, A_2, A_3), 3 small mass (B_1, B_2, B_3), 3 encoders (C_1, C_2, C_3) and a large central mass (D), as shown in Figure C.1. The central mass was supported and constrained by lead springs connected with actuators. In this thesis, only actuator (A_1) is used to control the position of corresponding small mass (B_1). Thus, the system is considered as single input a single output system.

The continuous controllers, after being discretized by Matlab, are implemented in the National Instrument environment which consists of Labview 2018 for software and NI CompactRIO for the hardware. Labview real-time control is used to read out the position measurement from the encoder and send an electrical signal to the actuator. The process is as follows. Firstly, the digital to the analogue module of the CompactRIO (NI9263) sends a control signal to the actuator through the amplifier. Then, the position information of the plant retrieved by the encoder is sent to the digital input module. Moreover, the encoder has a resolution of $100nm$. The schematic diagram of the setup is shown in Figure C.2.

C.2. Identification

In order to obtain the transfer function from the actuator signal to x displacement of the plant, the system identification experiment is carried out by inputting chirp signal to setup. The chirp signal composes of sinusoidal waves with increasing frequency by 2% every 0.1 second from 1 to 1000 Hz. The input and out signal in time range is shown in Figure C.3. The response is logged for every $50\mu s$ and the data is used to obtain the frequency response of the system using $tfestimate$ function by MATLAB. The open loop frequency response

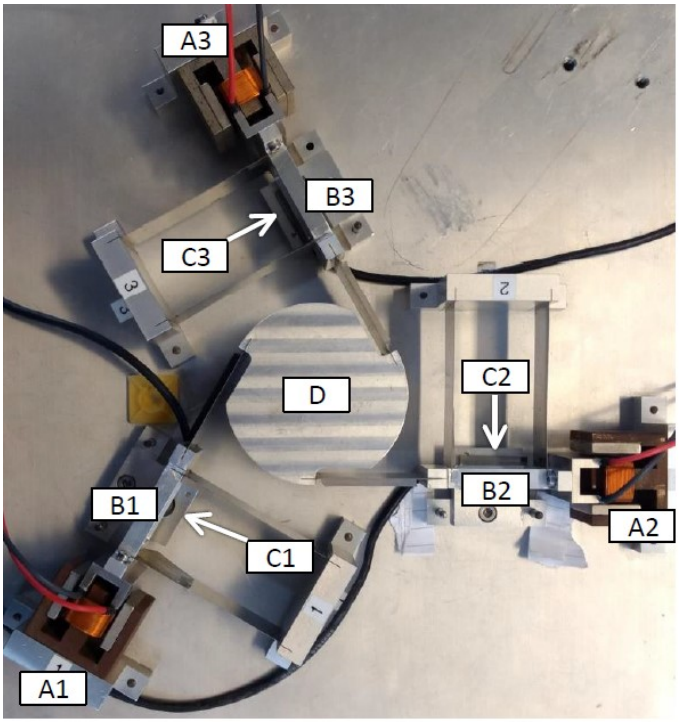

Figure C.1: The 3-DOF precision positioning stage

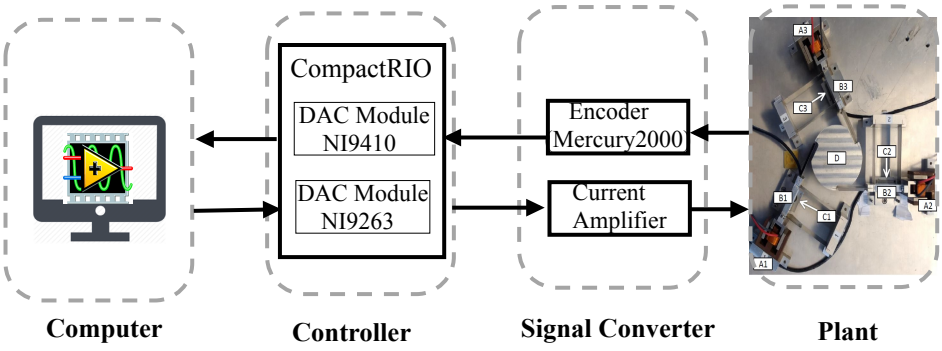

Figure C.2: Schematic overview of the experimental setup

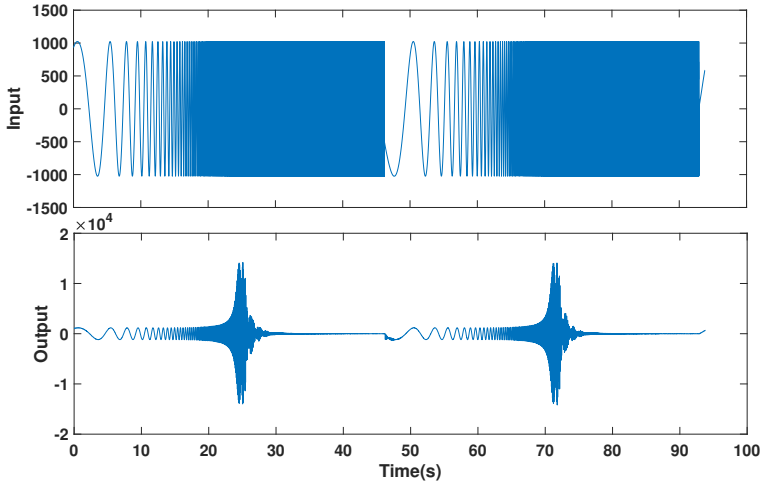

Figure C.3: Time response (output) of the plant from chirp signal(input)

of the system is shown in Figure C.4. From the result, the system can be considered as a single mass spring damper system and the estimated transfer function is obtained as follows:

$$P_{est}(S) = \frac{9602.5}{s^2 + 4.2676s + 7627.3} \tag{C.1}$$

C

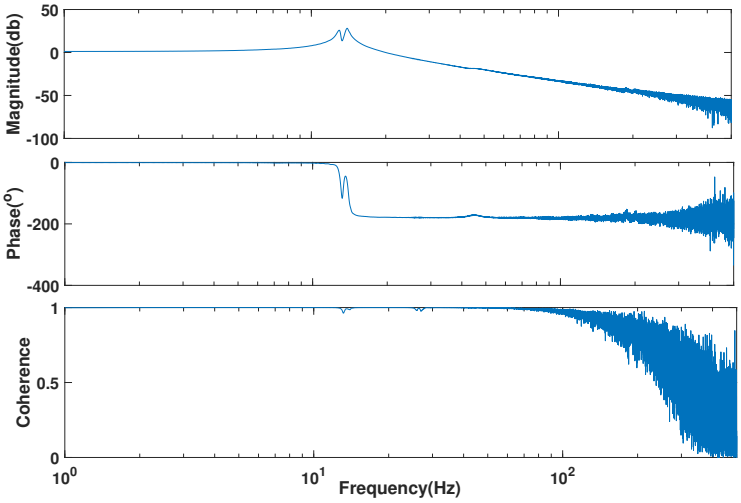

Figure C.4: Frequency response with coherence

D

Matlab Code and Simulink Model

In this appendix, the MATLAB and SIMULINK codes used in this thesis are given.

D.1. identification.m

This code is used to identify the transfer function from the data obtained from experiment.

```
data=load('system_identification.lvm');%load data obtained in the ...
    expriment

Ts=0.5e-4;        %sampling time
ip=da(:,1); %acquire ip data
op=da(:,2);%acquire op data

% identification analysis
[T,f]=tfestimate(ip,op,[],[],[],1/Ts);
[C,f]=mscohere(ip,op,[],[],[],1/Ts);

%plot ip and op
figure;
time=1:size(ip);
time=time.*Ts;
subplot(211)
plot(time,ip)
ylabel('ip')
subplot(212)
plot(time,op)
xlabel('Time(s)');ylabel('op')
xlim([0 max(time)]);

%plot frequency response and coherenec
figure;
subplot(311)
semilogx(f,20*log10(abs(T)))
ylabel('Magnitude(db)')

```

```
subplot(312)
semilogx(f,rad2deg(unwrap(angle(T))))
ylabel('Phase(degree)')

subplot(313)
semilogx(f,C)
xlabel('Frequency(Hz)');ylabel('Coherence')
xlim([1 5e2])
```

D.2. hodf.m

This code is adapted from Kars Heinet's thesis. It is used to calculate the Higher Order Sinusoidal Describing Functions (HOSIDFs) of reset elements.


```
function [G] = hodf(sys,Ar,n,freqs)
%calculate high order describing function of FORE and SORE
%sys: state space matrix of linear base dynamics
%Ar: gamma
%n:the order of describing function(only odd number)
%freqs: the frequencies the describing function is calculated for
%A,B,C,D:state space matrix
if (mod(n,2)==0)
    G=0;
    return;
end
A=sys.a;
B=sys.b;
C=sys.c;
D=sys.d;
G=zeros(1,numel(freqs));
for i=1:numel(freqs)
    w=freqs(i);
    lambda=w*w*eye(size(A))+A^2;
    lambdainv=inv(lambda);
    Delta=eye(size(A))+ expm(A*pi/w);
    Delta_r=eye(size(A))+ Ar*expm(A*pi/w);
    gamma_r=inv(Delta_r)*Ar*Delta*lambdainv;
    theta_D=(-2*w*w/pi)*Delta*(gamma_r-lambdainv);

    if(n==1)
        G(i)=C*inv(j*w*eye(size(A))-A)*(eye(size(A))+ j*theta_D)*B+D;
    else
        G(i)=C*inv(j*w*n*eye(size(A))-A)*j*theta_D*B;
    end
end
if  (n==1)
    G=G+D;
end
```

D.3. secondCgLp_coefficient.m

This code is used to obtain the coefficient α_1 and α_2 in 2^{nd} CgLp elements.

```
%acqurire the coeffiecients for second order CgLp such that the gain ...
    is constant
%wra=100Hz and beta=1 are used as benchmark  for second order lead ...
    filter
%  a1=alpha_1  considers the shift of cutoff frequency  a2=alpha_2 ...
    consider the adjustment for the damping ration.
gamma=[0.9:-0.1:-0.9];
wra=100*2*pi; % benchmark of crossover frequency
beta=1;       % benchmark of damping ration
%the state matrix of 2nd order lead filter
A=[0   1;-(wra^2) -2*beta*wra];
B=[0;wra^2];
C=[1  0];
D=0;
sys=ss(A,B,C,D);
w=logspace(1,7,600);
lb = [0  0];% lower bound of coefficients
ub = [   ];
a0=[10  10];% initial coeffiecients
for n=1:1:numel(gamma)
            gamma(n)
        A_gamma=[gamma(n)  0;0    gamma(n)];
        alpha=@(a)max(abs(20*log10(abs(hodf(sys,A_gamma,1,w).
        *(((j*w/wra/a(1)).^2)+(2*j*w*beta*a(2)/wra/a(1))+1)))));
        [a,fval]=fmincon(alpha,a0,[],[],[],[],lb,ub)
end
```

D.4. cornerfrequency_coefficient.m

This code is used to obtain the coefficient b that is used to calculate the corner frequency ω_r of CgLp elements such that the required phase compensation is achieved at the crossover frequency.

```

%wr=wc/b ,wc is the crossover frequency that needs phase compensation.
%This is an inverse method to obtain wr
%It is noticeable that not all the reset configurations can provide the
%required phase compensation and the cases where fval output >1
% should be abandoned

clear all;
close all;
clc;
PM=40;        % required phase compensation, degree
wr=100*2*pi; % corner frequency of CgLp
gamma=[0.9:-0.1:-0.9];

resetelement=1;     %  1 for first order CgLp;2 for second order CgLp
if resetelement==1  %  first order CgLp mode
```

```
    a=[ ];              %  insert $alpha$
     for n=1:1:numel(gamma)
       gamma(n)
       wra=wr/a(n);
       sym=ss(-wra,wra,1,0);
       Del=@(w)abs(PM-rad2deg(angle(hodf(sym,gamma(n),1,w)
       .*((w*j/(wr)+1)))));
       lb = [0];
       ub = [ ];
       [w,fval]=fmincon(Del,wr,[],[],[],[],lb,ub)
       b(n)=w/wr;
     end

else if resetelement==2 % second order CgLp mode
beta=1;
a=[ ];                    % insert  alpha_q  and alpha_w

lb = [0];
ub = [];
  for n=1:1:numel(gamma)
     wra=wr/a1(n,1);
     A=[0   1;-(wra^2) -2*beta*wra];
     B=[0;wra^2];
     C=[1  0];
     D=0;
     sys=ss(A,B,C,D);
     A_gamma=[gamma(n)  0;0  gamma(n)];
     Del=@(w)abs(PM-rad2deg(angle(hodf(sys,A_gamma,1,w)
     .*(((j*w/wr).^2)+(2*j*w*beta*a(n,2)/wr))+1))));
     [w,fval]=fmincon(Del,wr,[],[],[],[],lb,ub)
     b(n)=w/wr;        % cases where fval>1 should be abandoned
   end
    end
end
```

D.5. setup_sensitivity.m

This code is used to run the real-time simulation of the system and plot the new error sensitivity functions.

```
clear all;
close all;
clc;
PM=;                    % required phase compensation, degree
wc=;                    % target frequency ,rad/s
m=1.0414e-04;
c=4.4443e-04;
k=0.7943;               % setup prameters
T_sample=2e-4;          % sampling rate
resetelement=1;         % 1 for first order CgLp;2 for second order CgLp
freq=logspace(0,3,100)
s=tf('s');

if resetelement==1  % first order CgLp mode
```

```
15      a=[];                % insert $alpha$
16      b=[];                % insert the crossover frequency coefficients
17                           % obtained from cornerfrequency_coefficient.m
18      gamma=[];            % inset the feasible range of gamma
19    for n=1:1:numel(gamma);
20        wr=wc/b(n);    %
21        wra=wr/a(n);    % corner frequency of GFORE in CgLp
22
23        sys=ss(-wra,wra,1,0);
24        sys1=tf([wra],[1, wra]);
25        Gd=c2d(sys1,T_sample,'tustin');
26        [A_r,B_r,C_r,D_r]=ssdata(Gd);       % discretized reset control ...
              parameters
27        A_gamma=gamma(n);
28        G=hodf(sys,gamma(n),1,wc); % DF of FORE at wc
29        Gwc=1/(m*(wc*i)^2+c*(wc*i)+k); %gain of the plant at wc
30        Gd0=(wc*i/wr+1);             %  gain of lead filter at wc
31        Gl=1/(wc*j/(5*wc)+1);        %  gain of  low pass filter at wc
32
33        Kp=1/abs(Gd0*G*Gwc*Gl);
34        L=Kp*(s/wr+1)/(s/(5*wc)+1);       % cotinuous linear controller
35
36        Ld=c2d(L,T_sample,'tustin');
37        [numLd,denLd]=tfdata(Ld,'v');    % discretized linear control ...
              parameters
38    for k=1:1:numel(freq)
39        freq_k=freq(k);
40
41        T_c=20;         % calculation period
42        T_S=15;         % steady state time
43
44        sim('setup_simulation');
45        load('error');
46
47        er(n,k)=mag2db(max(abs(error(2,:))));
48
49    end
50       figure(1)
51       semilogx(freq,er(n,:));
52       hold on
53
54  end
55
56  else if resetelement=2           % second order CgLp mode
57           a=[];
58           b=[];
59           gamma=[];
60
61  for n=1:1:numel(gamma);
62       wr=wc./b(n);
63       wra=wr/(a(n,1));  % corner frequency of GSORE at CgLp
64       beta=1;
65       beta_r=a(n,2)*beta;
66       A_gamma=[gamma(n) 0;0 gamma(n)];
67       A=[0    1 ; -wra^2    -2*beta*wra];
68       B=[0;wra^2];
69       C=[1  0];
```

```
70        D=[0];
71        sys=ss(A,B,C,D);
72        sys1=tf([1],[1/wra^2   2*beta/wra   1]);
73        Gd=c2d(sys1,T_sample,'tustin');
74        [A_r,B_r,C_r,D_r]=ssdata(Gd); % discretized reset control parameters
75
76        G=hodf(sys,A_gamma,1,wc);       % DF of sore at wc
77        Gwc=1/(m*(wc*i)^2+c*(wc*i)+k)
78        Gd0=((wc*i/wr)^2+2*beta_r*wc*i/wr+1); % gain of lead filter at wc
79        Gl=1/(wc*j/(5*wc)+1)^2;
80
81        Kp=1./abs(Gd0*G*Gwc*Gl);
82
83        D=((s/wr)^2+2*beta_r*s/wr+1)*Kp/(s/(5*wc)+1)^2;
84        Dd=c2d(D,T_sample,'tustin');
85        [numLd,denLd]=tfdata(Dd,'v');
86
87    for k=1:1:numel(freq)
88        k
89        freq_k=freq(k);
90        T_c=20;  % calculation period
91        T_s=15;  % steay state time
92        sim('setup_simulation');
93        load('error');
94        er(n,k)=mag2db(max(abs(error(2,:))));
95        end
96        figure(1)
97        semilogx(freq,er(n,:));
98
99    end
100   end
```

D.6. Simulink for Real-time Simulation

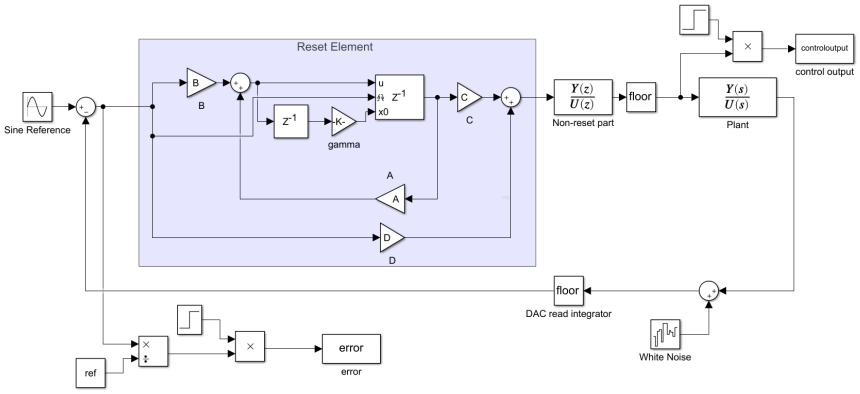

Figure D.1: Simulink schematic for real-time simulation named setup_simulation.slx

Bibliography

[1] WIKIPEDIA, "Defect(semiconductoe technology)." https://de.wikipedia.org/wiki/Defekt_(Halbleitertechnik), 2019. [web].

[2] K. J. Åström and T. Hägglund, "The future of pid control," *Control engineering practice*, vol. 9, no. 11, pp. 1163–1175, 2001.

[3] K. K. Tan, T. H. Lee, and S. Huang, *Precision motion control: design and implementation*. Springer Science & Business Media, 2007.

[4] S. Skogestad and I. Postlethwaite, *Multivariable feedback control: analysis and design*, vol. 2. Wiley New York, 2007.

[5] A. Baños, J. Carrasco, and A. Barreiro, "Reset times-dependent stability of reset control systems," *IEEE Transactions on Automatic Control*, vol. 56, no. 1, pp. 217–223, 2010.

[6] J. Clegg, "A nonlinear integrator for servomechanisms," *Transactions of the American Institute of Electrical Engineers, Part II: Applications and Industry*, vol. 77, no. 1, pp. 41–42, 1958.

[7] I. Horowitz and P. Rosenbaum, "Non-linear design for cost of feedback reduction in systems with large parameter uncertainty," *International Journal of Control*, vol. 21, no. 6, pp. 977–1001, 1975.

[8] L. Hazeleger, M. Heertjes, and H. Nijmeijer, "Second-order reset elements for stage control design," in *2016 American Control Conference (ACC)*, pp. 2643–2648, IEEE, 2016.

[9] L. Chen, N. Saikumar, and S. H. HosseinNia, "Development of robust fractional-order reset control," *IEEE Transactions on Control Systems Technology*, 2019.

[10] A. Vidal and A. Baños, "Reset compensation for temperature control: Experimental application on heat exchangers," *Chemical Engineering Journal*, vol. 159, no. 1-3, pp. 170–181, 2010.

[11] N. Saikumar, R. K. Sinha, and S. H. HosseinNia, "Resetting disturbance observers with application in compensation of bounded nonlinearities like hysteresis in piezo-actuators," *Control Engineering Practice*, vol. 82, pp. 36–49, 2019.

[12] L. Chen, N. Saikumar, S. Baldi, and S. H. HosseinNia, "Beyond the waterbed effect: Development of fractional order crone control with non-linear reset," in *2018 Annual American Control Conference (ACC)*, pp. 545–552, IEEE, 2018.

[13] A. Palanikumar, N. Saikumar, and S. H. HosseinNia, "No more differentiator in pid: Development of nonlinear lead for precision mechatronics," in *2018 European Control Conference (ECC)*, pp. 991–996, IEEE, 2018.

[14] S. H. HosseinNia, I. Tejado, and B. M. Vinagre, "Fractional-order reset control: Application to a servomotor," *Mechatronics*, vol. 23, no. 7, pp. 781–788, 2013.

[15] N. Saikumar, R. Sinha, and S. H. Hoseinnia, "'constant in gain lead in phase'element-application in precision motion control," *IEEE/ASME Transactions on Mechatronics*, 2019.

[16] Y.Salman, "Tuning a Novel Reset Element through Describing Function and HOSIDF Analysis." http://resolver.tudelft.nl/uuid:2236e1f6-4dc5-4f7f-96da-fc83ead69445, 2018.

[17] P. Nuij, O. Bosgra, and M. Steinbuch, "Higher-order sinusoidal input describing functions for the analysis of non-linear systems with harmonic responses," *Mechanical Systems and Signal Processing*, vol. 20, no. 8, pp. 1883–1904, 2006.

[18] K. Heinen, "Frequency analysis of reset systems containing a Clegg integrator: An introduction to higher order sinusoidal input describing functions." https://repository.tudelft.nl/islandora/object/uuid:ccc37af2-fcbc-46ec-9297-afdc5c1ea4b5?collection=education, 2018.